

Illinois State University

ISU ReD: Research and eData

---

Theses and Dissertations

---

2017

## Evaluating Relationships between Rock Strength and Longitudinal Stream Profile Morphometry in the Southern Guadalupe Mountains, Texas

Samuel T. Schoenmann

Illinois State University, Schoes34@gmail.com

Follow this and additional works at: <https://ir.library.illinoisstate.edu/etd>



Part of the [Geology Commons](#), and the [Geomorphology Commons](#)

---

### Recommended Citation

Schoenmann, Samuel T., "Evaluating Relationships between Rock Strength and Longitudinal Stream Profile Morphometry in the Southern Guadalupe Mountains, Texas" (2017). *Theses and Dissertations*. 774.

<https://ir.library.illinoisstate.edu/etd/774>

This Thesis-Open Access is brought to you for free and open access by ISU ReD: Research and eData. It has been accepted for inclusion in Theses and Dissertations by an authorized administrator of ISU ReD: Research and eData. For more information, please contact [ISUReD@ilstu.edu](mailto:ISUReD@ilstu.edu).

# EVALUATING RELATIONSHIPS BETWEEN ROCK STRENGTH AND LONGITUDINAL STREAM PROFILE MORPHOMETRY IN THE SOUTHERN GUADALUPE MOUNTAINS, TEXAS

Samuel T. Schoenmann

72 Pages

Landscapes record information about the tectonic, climatic, and lithologic environments in which they form (Yang et al., 2015). When one or more of these environmental conditions change spatially or temporally, the landscape responds through erosion and thus, develops representative geomorphic features (Ritter et al., 2011). Since the nineteenth century, it has been clear that bedrock strength and erodibility play an important role in landscape evolution and geomorphology (Lifton et al., 2009). However, the nuances of variable erodibility remain poorly understood. The implications of this limited understanding lies within landscape evolution models. While these models show strong qualitative relationships between longitudinal river profile morphometry and tectonic or climatic processes, major discrepancies remain over the relationship between bedrock strength and river incision. As these models strive to become more accurate, they are limited by our understanding of discrete characteristics of substrate erodibility. For this reason, the Southern Guadalupe Mountains are an excellent location to focus on these issues. Minor variations in carbonate lithology in this region will provide a focused insight on the relationships between discrete changes in bedrock strength, erodibility, and longitudinal stream profile morphometry. Additionally, this study is among the first to utilize longitudinal

stream profiles in the Southern Guadalupe Mountains, Texas with the intent to explore the landscape for tectonic and lithologic influences on landscape evolution.

Here, the relationships between rock strength and vertical river incision are explored using classic type-N Schmidt hammer analysis and longitudinal stream profiles obtained from digital elevation models. Qualitative exploration of longitudinal stream profiles in the Southern Guadalupe Mountains has revealed high-elevation, low-relief equilibrium profiles in the upstream segments of rivers crossing steep normal faults. It is likely that upstream, downthrown, hanging walls have produced mid profile pseudo-base levels in upper reaches of rivers by producing dam-like structures. Downstream of these structures, profiles are convex and show evidence for possible increased localized uplift rates, or significantly decreased erosional efficiency. Statistical results show that mean rebound values from type-N Schmidt Hammer analysis can be used to predict stream gradient, knickpoint development, and residual errors inherent in Flint's Law (river incision model) only under relatively simple tectonic and hydrologic regimes. These relationships do not hold true in circumstances where large confluences and/or faulting disrupts major stream channel networks, or in areas under topographic disequilibrium. Finally, geologic units with different, yet statistically similar rebound values were found to influence stream gradients differently. This suggests that lumping lithologies together based on similar rebound values is an overgeneralization and should be avoided.

**KEYWORDS:** Schmidt Hammer, Rebound, Rock Strength, Longitudinal Stream Profiles, Geomorphology, Southern Guadalupe Mountains, Flint's Law Residual Errors.

EVALUATING RELATIONSHIPS BETWEEN ROCK STRENGTH AND LONGITUDINAL  
STREAM PROFILE MORPHOMETRY IN THE SOUTHERN  
GUADALUPE MOUNTAINS, TEXAS

SAMUEL T. SCHOENMANN

A Thesis Submitted in Partial  
Fulfillment of the Requirements  
for the Degree of

MASTER OF SCIENCE

Department of Geography-Geology

ILLINOIS STATE UNIVERSITY

2017

© 2017 Samuel T. Schoenmann

EVALUATING RELATIONSHIPS BETWEEN ROCK STRENGTH AND LONGITUDINAL  
STREAM PROFILE MORPHOMETRY IN THE SOUTHERN  
GUADALUPE MOUNTAINS, TEXAS

SAMUEL T. SCHOENMANN

COMMITTEE MEMBERS:

Lisa Tranel, Chair

Eric Peterson

Jonathan Thayn

## ACKNOWLEDGMENTS

First, I would like to thank my advisor Lisa Tranel for her guidance and mentorship throughout my time at Illinois State University. From the Guadalupe Mountains to GSA conferences in Denver, CO, she has shown me how to think and present myself in a manner conducive to geologic research and academic scholarship. Second, I would like to thank my committee members; John Thayn, for providing invaluable support in statistics, coding, and out-of-the-box viewpoints; and Eric Peterson for his mentorship and capacity to provoke critical thinking. I am happy to have had their company and leadership to guide me through this program.

I would also like to thank undergraduates Kacey Garber, Jeremy Neundorff, Kirsten Schaefer, and Chad Cremer for their help and comradery in the field. Their efforts and detailed field notes were central to the completion of this thesis.

A special thanks as well for my fellow graduate classmates whom provided necessary feedback, criticism, and friendship as we each progressed in our field. Lastly, I would like to thank the ISU Department of Geography-Geology for their abundant resources including graduate assistantships, job outreach, and the capability of providing a wholesome environment in which to grow. I will always revere my mentors, and forever hold this experience as the most invaluable accomplishment of my career. Thank you all for your support.

S. T. S.

## CONTENTS

	Page
ACKNOWLEDGMENTS	i
CONTENTS	ii
TABLES	iv
FIGURES	v
CHAPTER	
I.    INTRODUCTION AND OBJECTIVES	1
Introduction	1
Research Objectives	4
Research Questions and Hypotheses	5
Questions	5
Hypotheses	6
II.   BACKGROUND	7
Study Site: Southern Guadalupe Mountains	7
Stratigraphy	11
Back-Reef	11
Reef	12
Fore-Reef and Basin	12
Rock Strength	15
Longitudinal Stream Profiles	15
Flint's Law	20
III.  METHODOLOGY	24
Rock Strength Analyses	24
Schmidt Hammer Analysis	24
Rock Mass Strength Analysis	28
Delineating Stream Profiles	30
Delineating Mechanisms for Knickpoint Development	31



Application of Flint's Law	31
Data Analysis	32
IV. RESULTS	35
Rebound and Erodibility between Geologic Units	35
Relationships between Rebound and Stream Gradient/Knickpoints	39
Relationships between Rebound and Flint's Law Residual Errors	42
V. DISCUSSION	45
Rebound and Erodibility	45
Stream Gradient and Knickpoint Development	47
Flint's Law Residual Errors	56
Future Improvements and Sources of Uncertainty	57
VI. CONCLUSION	59
REFERENCES	61
APPENDIX A: Study Site with Knickpoints, Sample Sites, and Geology	65
APPENDIX B: King's 1948 Geologic Map Symbols Key	66
APPENDIX C: Master Rebound Tables	67
APPENDIX D: Stream Gradient vs Flint's Law Residual Errors	68
APPENDIX E: Rebound vs Stream Gradient w/ Scatter	69
APPENDIX F: Rebound vs $K_{sn}$ w/ Scatter	70
APPENDIX G: Rebound vs Flint's Law Residual Error w/ Scatter	71
APPENDIX H: Stream Delineation Steps in GIS (ver. 10)	72

## TABLES

Table	Page
1. Flint's Law Regression Analysis	34
2. Rebound Weighted Means/STDV	36
3. Rebound vs RMS Regression Analysis	37
4. Rebound vs $K_{sn}$ Regression Analysis	37
5. Rebound vs Stream Gradient Regression Analysis	40
6. Rebound vs Residuals Regression Analysis	43

## FIGURES

Figure	Page
1. Image Comparing the Location of the Southern Guadalupe Mountains to Other Physiographic Provinces	8
2. Map of study area showing McKittrick and Pine Springs Canyons	10
3. Stratigraphy of the Delaware Basin and Guadalupe Mountains	14
4. Mechanisms for Knickpoint Development	17
5. Equilibrium Longitudinal River Profile Influenced by Karst Landscape	20
6. Log Slope – Log Area Regression Plot and Error	23
7. Map of Rock Strength Study Sites in Pine Springs and McKittrick Canyons	27
8. Influence of Structural Joints on Plucking	29
9. Weighted Mean Rebound per Geologic Unit with Standard Deviations	36
10. Regression Analyses between Rebound and Normalized Steepness ( $K_{sn}$ )	38
11. Regression Analyses between Rebound and Channel Gradient (Slope)	41
12. Regression Analyses between Rebound and Flint's Law Residual Errors	44
13. MC5 Longitudinal Stream Profile	48
14. MC10 Longitudinal Stream Profile	50
15. PS1 Longitudinal Stream Profile	51
16. MC1 Longitudinal Stream Profile	53
17. MC1 Stream Profile Interpretation from Faulting	54
18. Map of Study Area with the Distribution of Hillslope and Normalized Steepness	55

# CHAPTER I

## INTRODUCTION AND OBJECTIVES

### **Introduction**

Landscapes record information about the tectonic, climatic, and lithologic environments in which they form (Yang et al., 2015). When one or more of these environmental conditions change spatially or temporally, the landscape responds through erosion and develops geomorphic features that represent the respective change (Ritter et al., 2011). Since the nineteenth century, it has been clear that bedrock strength and erodibility play an important role in landscape evolution and geomorphology (Lifton et al., 2009). However, the nuances of variable erodibility remains poorly understood. The implication of this limited understanding lies within landscape evolution models. While these models show strong qualitative relationships between longitudinal river profile morphometry and tectonic-climatic processes, major discrepancies remain over the relationship between bedrock strength and river incision. As these models strive to become more accurate, they are limited by our understanding of discrete characteristics in substrate erodibility. For this reason, the Southern Guadalupe Mountains is an excellent location to focus on these issues. Minor variations of carbonate lithology in this region provide a focused insight on the relationship between discrete changes in bedrock strength, erodibility, and their effect on longitudinal stream profile morphometry. Additionally, this study is among the first to utilize longitudinal stream profiles in the Southern Guadalupe Mountains, Texas with the intent to explore the landscape for tectonic and lithologic influences on landscape evolution.

There are many benefits to understanding and predicting landscape evolution in mountainous terrain. Firstly, natural phenomena such as floods and debris flows commonly

affect human safety and infrastructural integrity and are inherently associated with channel gradient, or slope, and landscape evolution. Secondly, and as mentioned above, is the affinity for landscapes to record tectonic, climatic, and lithologic conditions of an environment (Wobus et al., 2006). Complex earth processes including tectonic plate dynamics and shallow mantle processes are aptly communicated on the Earth's surface through erosion. Patterns of erosion across a region can indicate when and where environmental changes occur.

In mountainous landscapes, the primary response to changing environmental conditions is river incision (Whipple, 1999; Burbank and Anderson, 2001; Ritter et al., 2011; Ellis et al., 2014). This is an important consideration due to the fact that rivers set the lower boundary condition at which adjacent hillslopes and ridges will erode. Therefore, rivers dictate the overall relief of a mountainous landscape (Whipple, 1999; Whipple, 2004) and are the focus of many landscape evolution models. When a landscape is in a state of equilibrium, erosion rates across the respective landscape are generally uniform or somewhat graded, and river channels tend to be concave up, with slope increasing in the upstream direction. When environmental conditions begin to change at a rate beyond the efficacy at which a river can erode and transport sediment, anomalous erosional patterns begin to develop (Sklar and Dietrich, 2001; Montgomery and Brandon, 2002; Anders et al., 2008; Allen et al., 2013). These anomalies are commonly identified as large convexities. In river or stream channels, these anomalous convexities are referred to as knickpoints, and have associations with multiple environmental factors including dynamic or variable tectonic regimes, climatic regimes, rock strength, and other complex conditions (Whipple, 1999; Burbank and Anderson, 2001; Ritter et al., 2011; Ellis et al., 2014). For these reasons, fluvial-geomorphology has become a common tool for geoscientists

conducting research that aims to identify recent patterns in climate change, tectonics, and predictive landscape evolution models (Wobus et al., 2006).

Of these models, Flint's Law for river incision is the most popular and is widely used for a myriad of studies (Wobus et al., 2006) that aim to predict the slope of longitudinal stream profiles. A common issue with this method, however, is the presence of "inherent" residual errors within the predictive results of this model. Several attempts have been made to correct these errors including Wobus et al.'s (2006) smoothing techniques, and Lu and Shang's (2015) integral approach; however, little consideration has been given to variations in channel gradient due to rock strength. Could an evaluation of these residual errors help enhance the predictive ability of landscape evolution models? This study aims to explore changes in bedrock strength and its influence on longitudinal stream profile morphometry in the Southern Guadalupe Mountains, Texas.

The Southern Guadalupe Mountains are located on the eastern margin of the north-south trending Rio Grande Rift in the American Southwest (Gao et al., 2004)(Figure 1A). Despite the relatively barren landscape, geologists have found several reasons to study this region. Most notable for his large contributions in geologic mapping and resource recovery, Phillip B. King produced the first high-resolution geologic map of the Southern Guadalupe Mountains in 1948. Since then, several studies have explored the stratigraphic history and structural characteristics of this region (Scholle and Halley, 1980; Standen et al., 2009). They have found the region to be widely dominated by reef forming carbonates that act as both source and reservoir rock for petroleum and that display characteristics of complex syndepositional and extensional tectonics (King, 1948; Standen et al., 2009). Additionally, gravity, density, and heat anomalies have been discovered in association with the Rio Grande Rift that might suggest the

presence of complex mantle processes related to mantle upwelling, down-welling, and lithospheric erosion (Figure 1A)(Gao et al., 2004; Rocket and Pulliam, 2011). Subsequently, this region serves as an ideal location to study surface expressions of complex mantle processes. While some studies have delineated the complex Oligocene-Miocene tectonic history of these mountains through speleological research in karst-cave networks near Carlsbad, NM (DuChene and Cunningham, 2006; Kosa and Hunt, 2006), more recent Pliocene to Holocene aged tectonic processes remain poorly constrained. However, newer research suggests that studies focusing on the geomorphology of large ( $>1 \text{ km}^2$ ) mountainous catchments could offer greater resolution to recent tectonic or climatic events in this region (Wobus et al., 2006; Ritter et al., 2011; Ellis et al., 2014).

Few studies have looked at the geomorphology of the Guadalupe Mountains for surficial expressions of tectonic or climatic signals. One example that has approached this topic, however, is a study by Hoffman (2014) that describes spatial variability of erosion in the eastern margin of the Guadalupe and Brokeoff Mountains. Hoffman (2014) identified knickpoints within longitudinal stream profiles and a distribution of areas with high-gradient versus low-gradient terrain. In Hoffman's (2014) study, areas that exhibited rapid lateral changes in gradient were speculated to have formed as a result of differential rock strength or the presence of faulting. Additionally high-gradient terrain was said to be eroding more quickly than low gradient terrain. However, a confident interpretation of these conclusions requires further scientific investigation.

### **Research Objectives**

We propose a small-scale study within McKittrick and Pine Springs Canyons of the Southern Guadalupe Mountains, in Guadalupe Mountains National Park (Figure 2), that re-

investigates longitudinal stream profiles derived using ArcGIS (v. 10) and orients them spatially with local changes in rock-type, rock-strength, and geologic structures such as folds and faults. Similar to Hoffman's (2014) study, we will examine the landscape of the Southern Guadalupe Mountains for rapid lateral changes in hillslope-gradient, but specifically focus on the geomorphology of longitudinal stream profiles, and how qualities including channel-steepness and concavity change spatially. Longitudinal stream profiles that contain knickpoints may be a result of faulting, uplift, subsidence, or climate change but are often times features that form simply due to differential rock strength (Wobus et al., 2006). If differential-rock strength is not a sufficient explanation for anomalous erosional features, then it is likely that one or several other aforementioned forces are either significantly contributing to, or dominating, landscape evolution in the Southern Guadalupe Mountains. We will also explore relationships between rock strength and residual errors within Flint's Law river incision models as applied to this region. We hope to delineate any relationships between rock strength, erodibility, stream gradient and residual errors to provide further insight into the importance of rock strength and landscape evolution as well as help reduce error in landscape evolution models.

## **Research Questions and Hypotheses**

### ***Questions***

- 1) Does rock strength and erodibility vary between King's (1948) geologic units?
- 2) Does rock strength explain channel gradient and knickpoint development?
- 3) Can rock strength predict residual errors in Flint's Law regression analyses?



### *Hypotheses*

- 1) Although the variation of lithology is limited within this region, we believe each rock type could contain variable rock strengths with predictable and correlative erodibility.
- 2) We expect stream gradient to increase with increased rock strength and knickpoints to develop at geologic contacts where the respective units have statistically significantly different rock strengths.
- 3) If rock strength does indeed affect stream gradient, we expect to see positive errors associated with harder rocks and negative errors associated with softer rocks.

## CHAPTER II

### BACKGROUND

#### **Study Site: Southern Guadalupe Mountains**

The Southern Guadalupe Mountain's unglaciated and relatively undeveloped terrain offers excellent conditions for conducting quantitative and qualitative investigations aimed at identifying patterns in erosion caused by rock strength, tectonics, or climate. The Guadalupe Mountains are located in southern New Mexico and western Texas on the eastern margin of the Rio Grande Rift. Results from the 1999-2001 La Ristra project (Figure 1A) suggest that this area has experienced increased mantle upwelling and crustal thinning, resulting in east to west extension with footwall and graben development (Gao et al., 2004). Parallel north-trending high-angle normal-faults with 1100-1200m of displacement (King, 1948) are observed outcropping approximately 960-2667m of Permian aged Delaware basin reef-stratigraphy that surrounds the Delaware Basin (Figure 1B)(Standen et al., 2009). Extension of the Rio Grande Rift and uplift of the Guadalupe Mountains was not uniform (Gao et al., 2004). Primary exhumation occurred around 30 to 20Ma (Gao et al., 2004) during Laramide orogenic events, followed by a secondary phase of uplift and extension between 11.3 to 3Ma (DuChene and Cunningham, 2006). The secondary phases correlate with high-angle Basin and Range normal faulting (Ward, 1991), sedimentation of the Ogallala formation (Hawley 1993), and vertical incision of rivers and caves that currently shape the Guadalupe Mountains (Kosa and Hunt, 2006). Other studies that examine large karstic features within these mountains have found that argon ages in alunite speleothem deposits suggest water elevations may have decreased due to

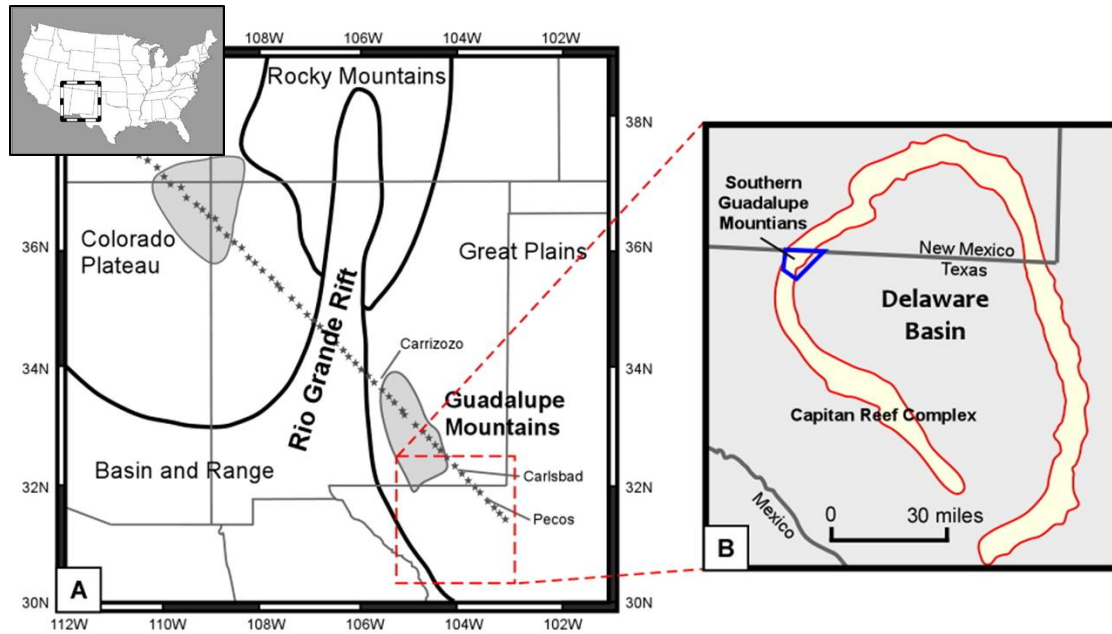


Figure 1: Image Comparing the Location of the Southern Guadalupe Mountains to Other Physiographic Provinces. A) Location of the Rio Grande Rift and Guadalupe Mountains. Stars represent research stations along the La Ristra project transect, (Modified from Gao et al., 2004). B) Location of the Southern Guadalupe Mountains in relationship to the Delaware Basin (Modified from Standen et al., 2009).

regional tilting, uplift, and secondary fault rejuvenation around 11.3 Ma., 6.0 to 5.7 Ma., and 4.0 to 3.9 Ma. (Polyak et al., 1998; Kosa and Hunt 2006).

Large escarpments with steep narrow catchments separate mountainous terrain on the east from the Great Salt Basin on the west. Catchments are generally larger than 15km<sup>2</sup> and shed water and sediments eastward from the north trending normal faults towards the Pecos River. This study takes place within the two largest canyons, Pine Springs and McKittrick Canyons, located in Guadalupe Mountains National Park (Figure 2). Pines Springs Canyon contains one major channel with several smaller tributaries. Faulting does occur near the lower portions of the main channel, but in association with quaternary alluvium (King, 1948). However it is unclear if these faults cross-cut the alluvium. Regardless, this tectonic and hydrologic regime is much

simpler when compared to McKittrick Canyon, which contains approximately three major stream channels, several tributaries, and steep normal faults that cross-cut bedrock in upper reaches of channels. Rivers with major channel confluences and exposed faults are referred to herein as having relatively complex hydrologic and tectonic regimes.

Field investigations reveal that the streams within these canyons are ephemeral in nature, existing sporadically through space and time, likely due to karst development and to low precipitation. Upper reaches of stream channels here commonly display drop blocks, slot canyons, and bedrock channels, while downstream reaches contain alluvial cover and boulder deposits. This suggests higher stream competency in upper reaches and decreased competency in lower reaches. Recent studies suggest that sediment transport and erosion rates are very low in this region (Happel et al., 2017), likely due to arid or semi-arid climatic conditions. Therefore, active incision and sediment transport most likely occur in upper reaches of stream segments and during low-frequency flood events (Reid et al., 1998).

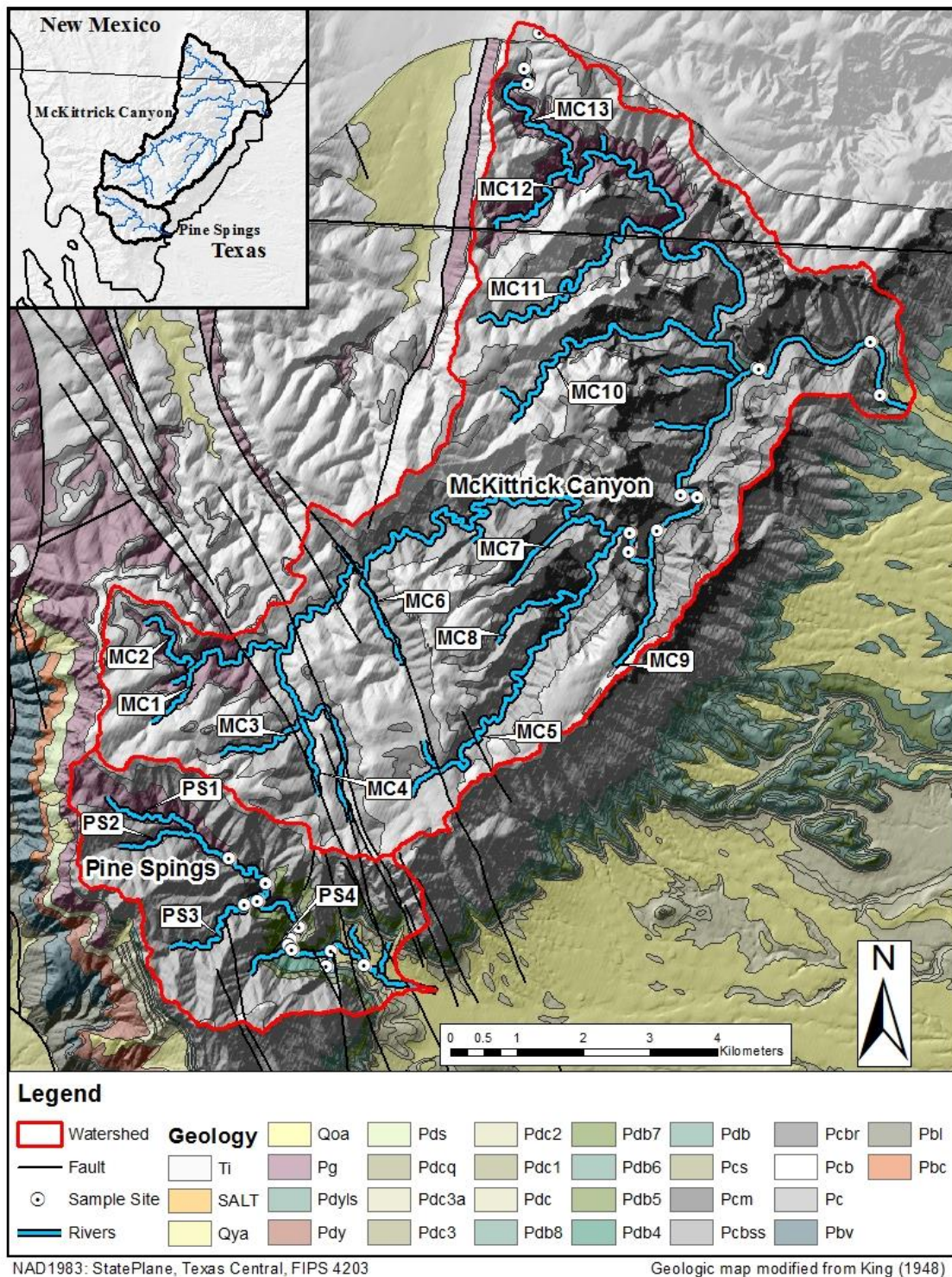


Figure 2: Map of Study Area Showing McKittrick and Pine Springs Canyons. Map contains King's (1948) geologic units, and the rock strength sites/ivers for this study.

## **Stratigraphy**

The Southern Guadalupe Mountains offers an excellent opportunity to observe intercontinental marine shelf-margin stratigraphy. Canyons within these mountains outcrop the eastern edge of the Permian-aged Delaware Basin carbonate reef complexes that grade laterally into distinct back-reef, reef, fore-reef, and basin members with marine carbonate deposits, intermittent terrigenous sandstones, and evaporites (Figure 2)(King, 1948; Scholle and Halley, 1980; Standen et al., 2009). Facies described here are part of a large carbonate reef system that rims the entire Delaware Basin (Figure 1b)(Standen et al., 2009).

### ***Back-Reef***

During the Permian, large intertidal lagoons trapped highly saline marine waters that resulted in the deposition of thinly bedded, fine-grained, fossiliferous limestones (Scholle and Halley, 1980). Decreased tidal connection resulted in high magnesium concentrations that consequently led to the dolomitization of several carbonate units (King, 1948). Several studies have shown that glaciation and eustatic sea-water fluctuations affected this region, resulting in high-stand and low-stand sedimentary sequences (King, 1948; Scholle and Halley 1989; Standen et. al., 2009). During high-stands, marine processes generated carbonate material and rivers deposited thin layers of sandstone. When sea-level fell, high-salinity shallow pools deposited packages of evaporites. In the Guadalupe Mountains, these units dip eastward by approximately 3-degrees, are well cemented, and increase in thickness and dip as they extend eastward. King (1948) initially categorized the back-reef units as the Carlsbad Limestone, but these have since been separated by sequence stratigraphy into the Greyburg, Queen, Seven Rivers, Yates, and Tansil formations. Moving basin-ward, limestone units transition to fossiliferous grain-limestones that contain prominent pisolites, in association with “teepee deposits,” that commonly

mark an exposed shelf crest, thickening beds, and increasing gradients which together mark the transition from back-reef to reef depositional environments.

### ***Reef***

The reef structures within these mountains are commonly massive, light colored fossiliferous limestones that grade into back-reef and fore-reef facies. The grade to back-reef is typically gradual, whereas the gradation to fore-reef is abrupt and easy to identify. This transition zone is defined as the Capitan Reef Complex and includes the Carlsbad, Capitan, and Goat Seep Members. The Capitan and Goat Seep Members are widely fossiliferous lime-boundstones that are largely continuous with occasional “spur-and-groove” channel morphologies (Scholle and Halley, 1980). The Capitan Reef deposits display the largest faunal diversity consisting of calcareous sponges and blue-green algae as framework organisms, and encrusting organisms such as bryozoans, brachiopods, echinoderms, mollusks, ostracods, corals, and trilobites (Scholle and Halley, 1980). Heavy calcareous aragonite and Mg-rich calcite cementation has greatly reduced porosity. Cementation of this unit is also believed to be pervasive, having occurred penecontemporaneously with sedimentation (King, 1948; Scholle and Halley, 1980). However, Capitan limestone lacks framework carbonates that would be capable of withstanding aggressive wave action (King, 1948; Scholle and Halley, 1980). As a result, heavy storms pulverized and brecciated the reef, sending debris downslope into deeper water.

### ***Fore-Reef and Basin***

The reef-slope contains in-situ sediments; however, the majority of sediments here derive from brecciated reef and near-reef rubble (Scholle and Halley, 1980). Members of the reef-slope range in thickness from a few to tens of meters and dip basinward at angles in excess of 35-degrees, before leveling out and growing thinner near the slope-base (King, 1948; Scholle and Halley, 1980; Standen et al., 2009). King (1948) classified these facies as massive light colored



brecciated limestone. They are well cemented and easily identified by their texture. The slope downgrades into clastic Bell Canyon and Cherry Canyon members of interfingering, thinly-bedded limestones, fine-grained sandstones, coarse-grained siltstones, and turbidite sequences that extend basinward. Carbonate units that enter the basin commonly thin and pinch-out, causing an abrupt contact between facies and sedimentological capstones. During eustatic regression cycles, terrigenous sediment bypassed back-reef and reef members and accumulated at the toe of the reef and within the basin as thin interbedded organic limestones, turbidites, and silty sandstones in the Brushy Canyon, Cherry Canyon, Bell Canyon, and Castile Formations.

Today, the majority of these units are visible along large western escarpments of the Guadalupe Mountains, however, the areas of concern, McKittrick and Pine Springs Canyons, outcrop varying members as their channels meander eastward into the Trans-Pecos Basin.



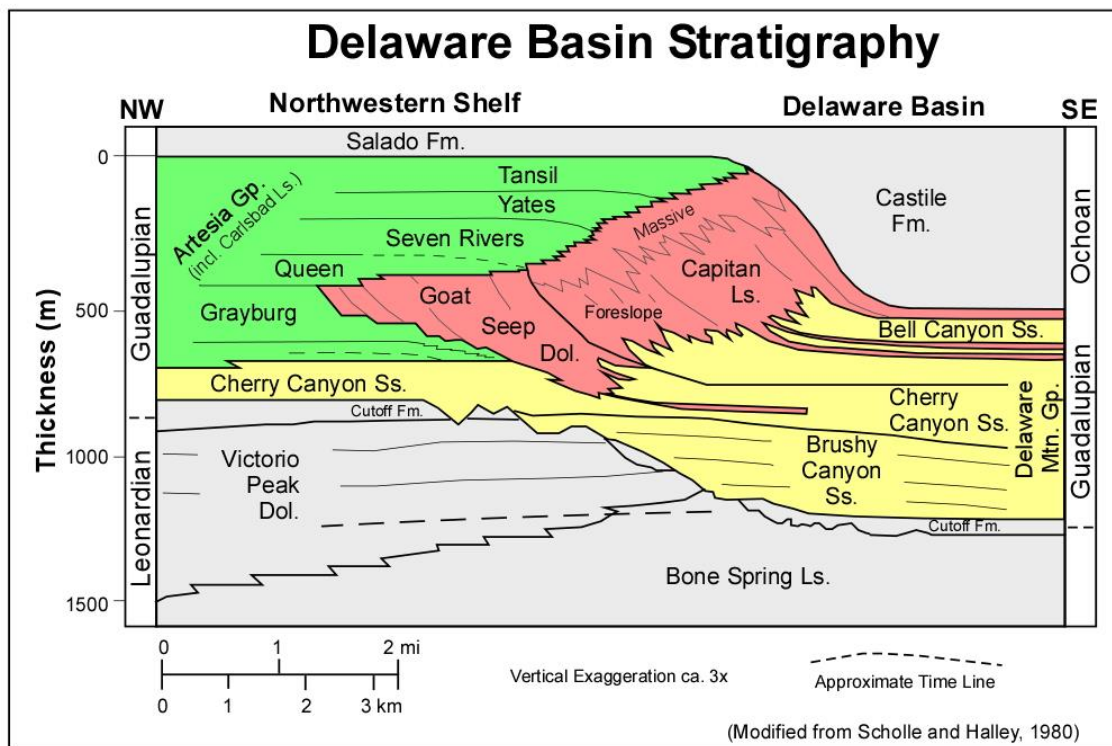


Figure 3: Stratigraphy of the Delaware Basin and Guadalupe Mountains. The Guadalupe Mountains consist predominantly of Guadalupian Group facies.

## **Rock Strength**

Rock strength, as described here, is a rock's general resistance to erosion. While the strength of a geologic rock-type holds a landscape in place, gravity, weathering, and erosion works to degrade the landscape (Whipple, 1999; Duvall et al., 2004; Larson and Montgomery, 2012). This is consistent with studies that show a significant positive relationship between rock strength, hillslope (Selby, 1980), and other geomorphic characteristics including channel width and sinuosity (Viles et al., 2011). In general, increasing rock strength generally leads to lower erodibility and, on occasion, over-steepened slopes (Selby, 1980; Selby, 1982). For this reason, rock strength is an important aspect to consider while studying landscape evolution and geomorphology. In terms of the Guadalupe Mountains, we focus on the mechanical rock strength of intact bedrock. Since this region is characterized by arid to semi-arid climate, we believe chemical erosion of bedrock is negligible, and will not greatly affect any results or interpretations made from mechanical rock strength measurements.

## **Longitudinal Stream Profiles**

All rivers tend toward a state of equilibrium that balances channel forming processes like erosion and transport with channel variables such as width, depth, and slope (Burbank and Anderson, 2001; Ritter et al., 2011). For example, a river or river segment that experiences relatively higher discharge and erosion rates will commonly display narrow and steep channels. The opposite is true however, for rivers and river segments with relatively lower discharge and erosion rates (Whipple 1999; Ritter et al., 2011). The balance between channel forming processes including discharge, erosion, or sediment entrainment and the expression of them in channel morphology is often referred to as hydraulic geometry (Burbank and Anderson, 2001;

Ritter et al., 2011). Each hydraulic parameter working in a river is mutually independent upon each other. As one parameter changes, one or more of the others must respond in order to maintain what has been coined as a "quasi-equilibrium" (Ritter et al., 2011). Moreover, bedrock-rivers exhibit a first-order response of mountain ranges to changes in uplift and climate by incising the landscape (Wobus et al. 2006; Allen et al., 2013). Rivers set a lower boundary condition (elevation) for adjacent hillslopes to erode. Thus, rivers control the relief and texture of the surrounding landscape (Ellis et al., 2014). The expression of these processes can be seen in both the vertical and horizontal aspects of river morphologies.

A common way to examine the geomorphology of rivers or streams is with longitudinal stream profiles. Longitudinal stream profiles represent the elevation and slope of a riverbed over distance. Rivers or river segments that have reached a state of quasi-equilibrium will ideally produce longitudinal profiles that are concave up and become less steep further downstream from a drainage divide (Ritter et al., 2011)(Figure 4.A). The lower end of this profile grades to some relative base-level. Common base-levels include the flanks of a mountain range, a large water body, or sea-level. Erosion is greatest at the head of the channel where it is steepest, and slowly transitions downstream into a depositional regime where gradients are not as steep.

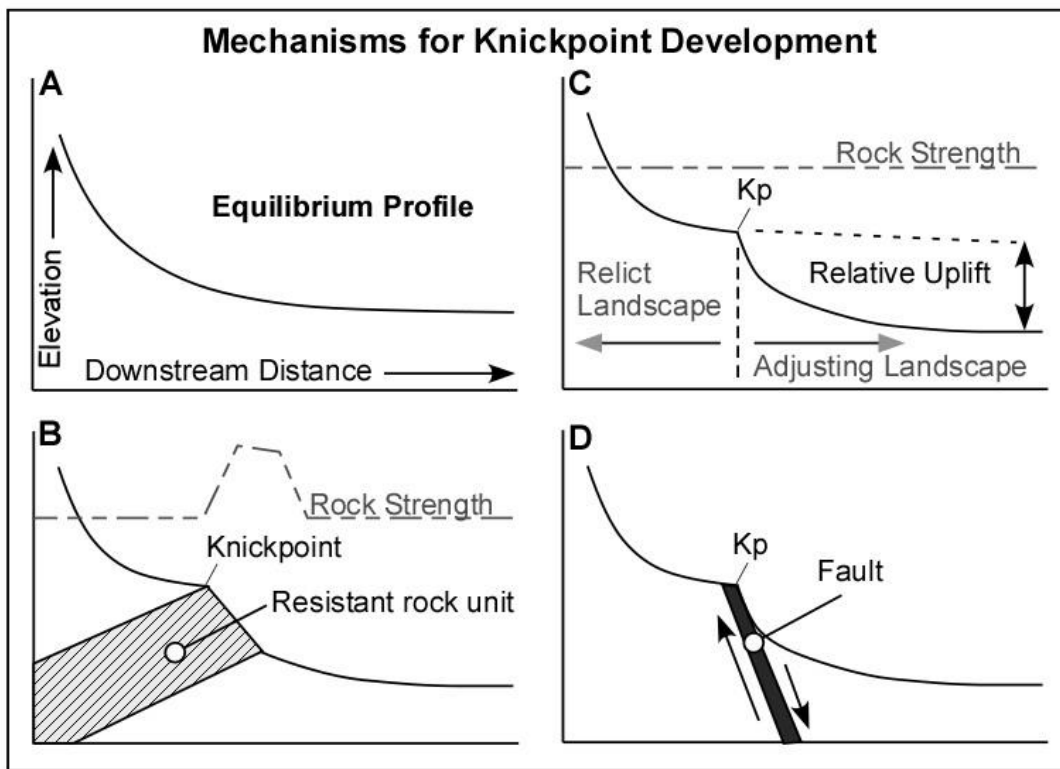


Figure 4: Mechanisms for Knickpoint Development. A) Equilibrium river profile. B) River profile with lithologic influence-increases in rock strength correlate with knickpoint development. C) Development of a migratory knickpoint (Fig. 5) from a relative drop of base level-note rock strength does not change. D) Faulting crosscuts a river channel and develops a knickpoint.

Disequilibrium conditions occur when a river is actively adjusting steepness and concavity to achieve a lower state of energy (Wobus et al., 2006; Ritter et al., 2011). Following a change in tectonic or climatic regimes, erosion begins at the origin of base-level adjustment and travels upstream leaving noticeable convexities, known as knickpoints (Figure 4A)(Whipple, 1999), in a longitudinal river-profile (Figure 4.B, C, and D). Over time, these knickpoints will completely traverse the length of the river, leaving behind a newly adjusted equilibrium profile (Ellis et al., 2014). Base-level change is relative and can occur under different circumstances:

1) Tectonic or Isostatic Uplift: in extensional settings like the Guadalupe Mountains, uplifting footwalls (horsts) form mountains and subsiding hanging walls (grabens) form basins. Rivers actively eroding the mountains adjust their equilibrium to surrounding basins, which act as a local base level. Mountains may rise, or basins may subside, thus lowering the base-level (Figure 4C). In this idealized scenario, we consider the uplift event to be large scale and thus adjusts the elevation of an entire catchment uniformly. Following this event, a knickpoint will develop at the site of faulting and travel upstream as a kinematic wave until stopped by a geologic force or reaches the drainage divide (Ouimet et al., 2009; Miller et al., 2013; Ellis et al., 2014).

2) Climate Change: Base-level can also be the elevation of a water body in which a river drains. In the extreme event that a highly wet environment is desertified, or there is a change in glacioeustatic sea-levels where sea-levels fall, water levels will decrease and result in a relative drop in base-level. The effects are similar to tectonic or isostatic uplift, where an erosional kinematic wave originates at the site of base-level adjustment and travels upstream (Ouimet et al., 2009). In both instances, a knickpoint will exist without any correlation to differential rock-strengths (Figure 4C).

3) Local Faulting: faulting may occur across a river channel and cut an ideal longitudinal river profile such that a knickpoint develops (Figure 4D). In this case, a small-scale change in base level occurs and the landscape must then compensate for the increased steepness by increasing erosion at the knickpoint. Longitudinal profiles and  $\log(S)$ - $\log(A)$  analysis will reveal a vertical step knickpoint that has similar channel gradients upstream and downstream of the convexity (Figures 4C and 4D)(Boulton et al., 2014).

As stated above, these types of knickpoints are, or may become, migratory features that originate at the location of base-level fall and attenuate upstream to the drainage divide (Whipple 1999). Additionally, in each of the above scenarios, a knickpoint can exist without any correlation to differential rock-strength. If this is the case, and the knickpoint is migratory in nature, the landscape is divided into two erosional regimes where rivers are actively adjusting to a new equilibrium below the knickpoint, and paleo/relict-landscapes above the knickpoint. These relict landscapes can contain evidence of tectonic or climatic conditions prior to the onset of knickpoint development (Whipple, 1999; Ellis et al., 2014).

While knickpoints commonly indicate that a landscape is in some state of disequilibrium, there are instances where they occur even though equilibrium has been achieved (Wobus et al., 2006). This often occurs where stream channels cross multiple geologic units with significant differences in erodibility. These knickpoints will develop on or near the geologic contact (Figure 4B)(Sklar and Dietrich, 2001). In carbonate environments, karstification and cave development has been found to result in knickpoint development at a swallet, where river processes such as erosion and sediment transport continue below the landscape in conduits, and again where the stream reappears at a spring (Figure 5)(Woodside et al., 2015). The knickpoint in this sense is somewhat misleading, due to the fact that river processes may actually continue underground in

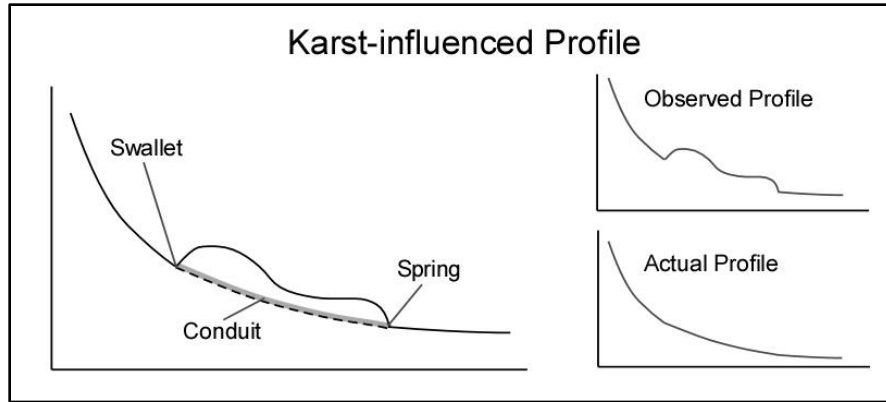


Figure 5: Equilibrium Longitudinal River Profile Influenced by Karst Landscape. Water is diverged into the subsurface at the swallet, where hydraulic processes occur underground until the water (or river) reemerges at the spring.

conduits rather than on the surface. The result is a longitudinal profile with a knickpoint at the location the river is lost to the subsurface, called a swallet. Normal surface processes then become apparent again where the stream reemerges through the respective spring (Woodside et al., 2015). Similar to faulting,  $\log(S)$ - $\log(A)$  regression analysis in these situations will commonly reveal a vertical step knickpoint. Although these instances do not necessarily allude to climatic or tectonic events, they are still integral for identifying geomorphic controls dictating landscape evolution in carbonate environments such as the Southern Guadalupe Mountains.

### Flint's Law

Flint's Law is a stream erosion model that estimates the slope at any given point in a river based on the upstream drainage area. Assuming topographic equilibrium conditions (*i.e. uplift and erosion rates are equal*), this relationship is described by the power equation:

$$S = K_n A^{-\left(\frac{m}{n}\right)} \quad (Eq. 1)$$

Where  $S$  is slope,  $K_n$  is a steepness index,  $A$  is area, and  $m$  and  $n$  are both positive constants related to basin hydrology. The ratio of  $m/n$  is commonly referred to as  $\theta$  and represents a concavity index. While slope( $S$ ) and area( $A$ ) are readily obtained from field measurements or DEM's (Wobus et al., 2006),  $K_n$  and  $\theta$  are difficult to measure and most easily estimated by rearranging Flint's Law and taking the  $\log_{10}$  of each side (Lu and Shang, 2015):

$$\mathbf{Log}(S) = -\theta\mathbf{Log}(A) + \mathbf{Log}(K_n) \quad (\mathbf{Eq. 2})$$

Here, we see that steepness indices and concavity are easily obtained with a simple regression line (Figure 6A) where the slope of the line is concavity ( $\theta$ ) and the y-intercept is the  $\log_{10}$  of our steepness index ( $K_{sn}$ ). However, with any regression analysis, there exists residual error where negative errors represent an over-prediction of stream gradient and positive errors represent an under-prediction (Figure 6b). Several studies have classified these errors as “inherent error” (Wobus et al., 2006), which result from DEM-processing limitations such as low DEM resolution resulting in step-like features in stream profiles. However, more work could be done to identify the cause of these errors and essentially answer the question: “Why do residual errors exist within Flint's Law regression analysis?” Nonetheless, Flint's Law has proven to be useful in identifying steepness indices ( $K_s$ ) and concavities ( $\theta$ ) of stream profiles (Wobus et al., 2006).

Once  $K_s$  and  $\theta$  are derived, it is common practice to calculate a regional average concavity index ( $\theta_{ref}$ ) using the average concavity for a determined region. This index ( $\theta_{ref}$ ) is then used to calculate normalized steepness indices ( $K_{sn}$ ) with the equation:

$$\mathbf{K}_{sn} = \mathbf{SA}^{\theta_{ref}} \quad (\mathbf{Eq. 3})$$

This value can be calculated for any given point along a stream profile, which is useful for qualitative identification of spatial patterns in uplift and bedrock erodibility (Ellis et al., 2014; Lu



and Shang, 2015). The relationship between uplift, erodibility, and  $K_{sn}$  is shown by the expression:

$$K_{sn} = \left(\frac{U}{K}\right)^{\frac{1}{n}} \quad (Eq. 4)$$

Where  $K$  is a dimensional coefficient for erosion efficiency and  $n$  is a positive constant related to regional hydrology. This suggests increases in  $K_{sn}$  represents conditions where uplift overwhelms erosional processes, or  $K$  significantly decreases.

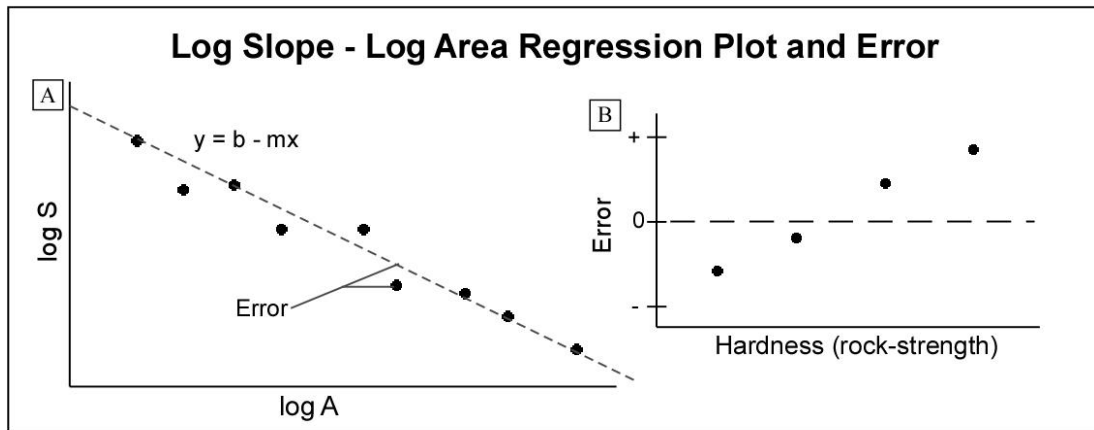


Figure 6: Log Slope – Log Area Regression Plot and Error. (A) Analysis typically reveals a negative linear trend in equilibrium river segments where the y-intercept (b) represents a steepness index and the slope (m) of the trend line represents a concavity ( $\theta$ ). Black dots represent actual data points from DEMs. (B) Errors between the regression line and data points may correlate with other attributes like rock strength, for example. Graph on the right portrays a hypothetical positive correlation between error and rock-strength.

## CHAPTER III

### METHODOLOGY

This study utilizes two categories of data: 1) rock strength, and 2) longitudinal stream profile morphometry. Rock strength data were collected in the field from bedrock exposures using the type-N Schmidt hammer and through rock mass strength (RMS) analysis. Channel morphometries including channel gradient, drainage area, elevation, and channel length were collected using digital elevation models (DEMs). Additionally, Flint's Law was applied to equilibrium reaches of stream channels to calculate a regional mean concavity ( $\theta_{\text{ref}}$ ) and a distribution of normalized channel steepness indices ( $K_{\text{sn}}$ ). Data processing was conducted qualitatively through visual correlation, as well as quantitatively (or statistically) with codes written in R.

#### **Rock Strength Analyses**

##### ***Schmidt Hammer Analysis***

The type-N Schmidt Hammer is a portable device that indirectly estimates the elastic deformation or uniaxial compressive strength of intact bedrock (Selby, 1980); otherwise known as mechanical rock strength. This device is inherently non-destructive and works by delivering a controlled, spring loaded, hammer-blow to the surface of intact bedrock to obtain a hammer-rebound value. Rebound values will increase as rock strength increases (Selby, 1980). Common practice is to average approximately 20+ rebound values for one overall rebound value. The number of strikes can be reduced if the standard deviation between strikes falls below  $R_{\text{stdv}} \pm 5$  (Selby, 1982; Basu, 2004; Ellis et al., 2014). Overall bedrock rebound values that are within one

standard deviation from each other are considered statistically similar in terms of rock-strength, while those exceeding one standard deviation of difference are considered statistically different (Ellis et al., 2014). Although lacking empirical evidence, the assumption is that two rocks with similar rebound values should exhibit similar erodibilities. Simple qualitative observation of landscape morphometry at geologic contacts can alleviate uncertainties associated with this assumption.

Twenty-four sample sites were selected for Schmidt Hammer analysis across the Southern Guadalupe Mountains to cover the range of King's (1948) geologic units that outcrop within stream channels of Pine Springs and McKittrick Canyons (Figure 7). Each hammer-strike was taken normal to bedrock-surface and was spaced a minimum of 3cm from previous strikes. Since the magnitude of hammer rebound is subject to influence from gravity, corrections were made to finalized rebound values based on the condition that strikes were made either vertically or horizontally. At each location, approximately 20 measurements ( $n=20$ ) were taken on both unpolished and aluminum-carbide-polished bedrock surfaces. At each site, these twenty measurement were used to estimate a single rebound value ( $x$ ). These measurements were then combined using a weighted mean (Equation 5), and weighted standard deviation (Equation 6):

$$\bar{x} = \frac{\sum_{i=1}^n (x_i * n_i)}{\sum_{i=1}^n (n_i)} \quad (Eq. 5)$$

$$wstdv = \sqrt{\frac{\sum_{i=1}^n n_i (x_i - \bar{x})^2}{\sum_{i=1}^n (n_i) - 1}} \quad (Eq. 6)$$

Where  $x$  is the rebound value for the “ $i^{th}$ ” measurement, and  $n$  is the number of strikes to obtain the respective rebound value ( $x$ ). This method accounts for the variability of overall rebound values at each location, as well as the variability between weathered, micro-fractured, and polished surfaces (Lifton et al., 2009). Since this study focuses on the influence of bedrock-

strength in fluvial settings, sampling was constrained to the bottoms and banks of stream channels. The correlation between rock strength and erodibility are compared using simple regression analyses, where rebound represents rock strength and  $K_{sn}$  and RMS-values represent erodibility.

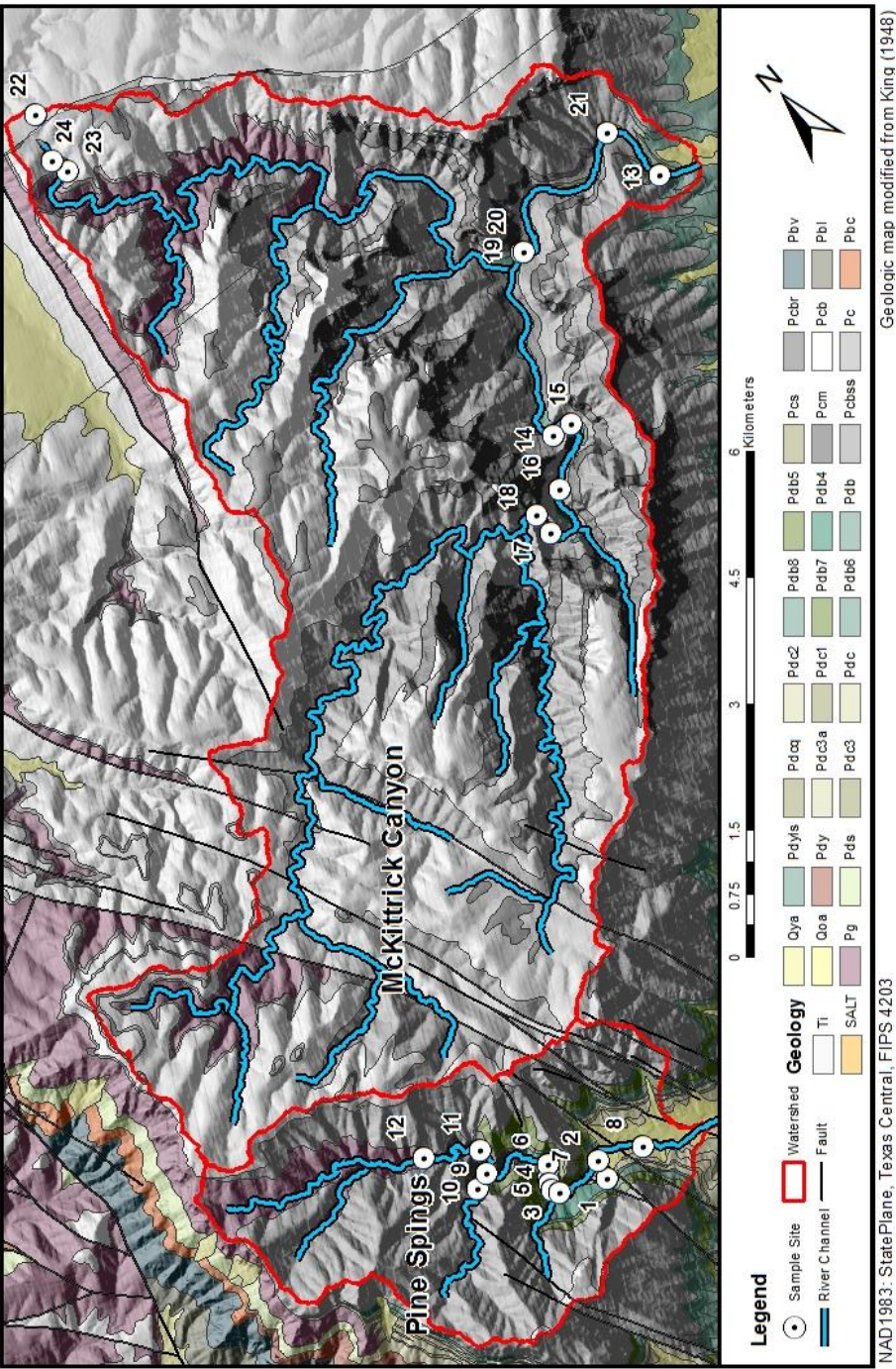


Figure 7: Map of Rock Strength Study Sites in Pine Springs and McKittrick Canyons. Depicted is King's (1948) lithologic units, known faults, and rock strength sample sites.

### ***Rock Mass Strength Analysis***

The second method used to estimate rock strength was the rock mass strength analysis (RMS), which grades *in-situ*, exposed bedrock on a scale of 1 (very weak) to 100 (very strong)(Selby,1982). Selby (1982) found this to be an effective method in predicting the steepness of hillslopes comprised of sedimentary lithologies. This method utilizes rebound values from Schmidt hammer analyses combined with additional field observations. These additional observations include: (1) the apparent degree of bedrock weathering, (2) joint size, (3) joint spacing, (4) joint fill, (5) joint or bedding orientation with respect to hillslope, and (6) the presence of groundwater flow (Selby, 1980; Moon et al., 2001; Moore et al., 2011). Each category (weathering, jointing, etc.) is weighted in proportion to its specific influence on outcrop stability, with joint spacing and joint orientation being the most significant variables (Selby, 1982). For example, weak rock might display closely spaced joints that dip steeply out of the hillslope or river channel, allowing loose fragments to become easily dislodged (Figure 8A). Stronger rocks either will lack jointing, or have widely spaced joints that dip into the hillslope, creating a scenario where loosened fragments are not as easily removed from the outcrop (Figure 8B).

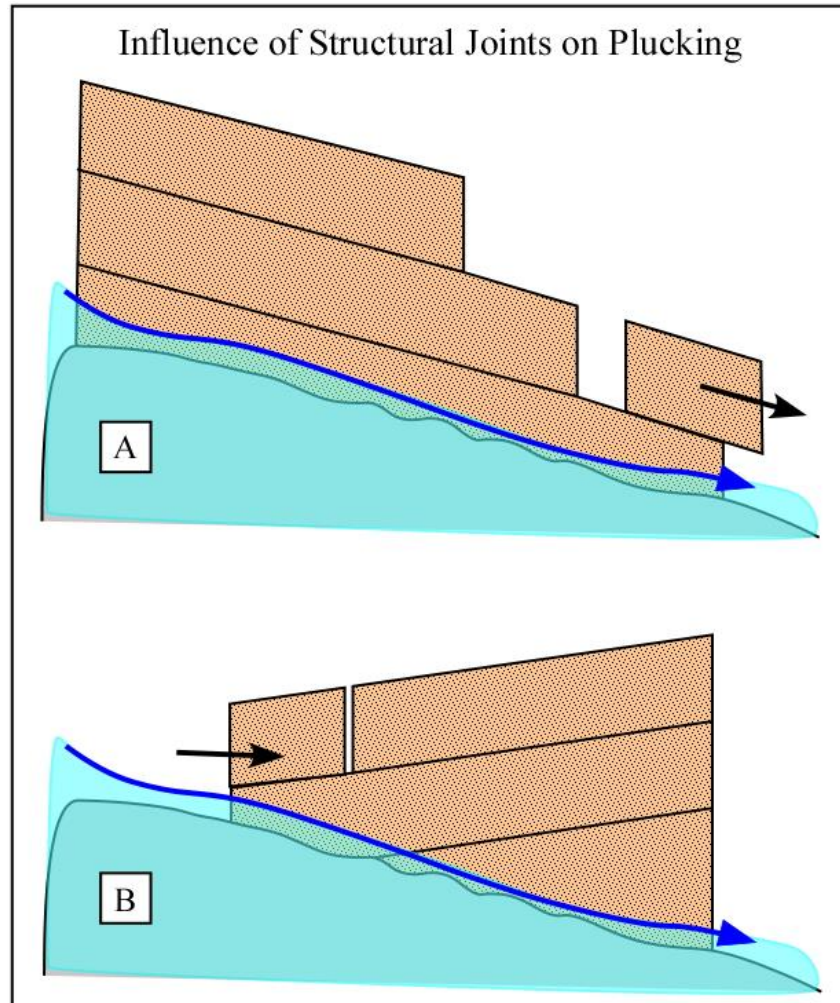


Figure 8: Influence of Structural Joints on Plucking. (A) Diagram of beds or jointing planes that dip out of a channel, versus (B) beds or jointing planes that dip into a channel.



Twelve sample locations (Figure 7) were chosen across the Southern Guadalupe Mountains, with six in Pine Springs Canyon and six in McKittrick Canyon. These analyses do not cover the full range of geologic units outlined by King (1948). However, these samples were chosen to affirm the validity of Schmidt hammer results in assessing erodibility. Additionally, and similarly to the method chosen for Schmidt hammer sample collection, RMS measurements were constrained to stream channel bottoms and banks. The area examined at each location varied in size because bedrock exposures are not consistent through each canyon. Rather, whole outcrops were considered at each location to assess the degree of weathering and jointing at each site. Joint orientation was measured using a Brunton compass, and joint width, spacing, continuity, etc. were measured with metric tapes and rulers. Methods for conducting measurements and weighting each was carried out in concordance with Selby's (1980) field methods.

### **Delineating Stream Profiles**

Longitudinal stream profiles were delineated using model builder in ArcGIS (v. 10) and freely available 10-meter DEMs acquired from the US Geological Survey 3D Elevation Program (3DEP). Seventeen stream channels with at least 1-km<sup>2</sup> contributing drainage area were selected from McKittrick and Pine Springs Canyons. Following methods in Wobus et al. (2006), stream channel data were resampled at equal intervals of 10m-elevation (original contour interval) to smooth profiles and reduce data "noise." Slope and upstream meandering channel distance were calculated using the DEM's resampled topographic data. Flow accumulation (upstream drainage area in square meters) was added to the resampled stream points and used in combination with slope for further processing in Flint's Law (Equation 1). Furthermore, knickpoints were

identified within stream profiles. Knickpoints were identified here as areas with anomalously high slopes, or slope breaks, where there is a rapid rejuvenation of slope in the downstream direction.

### **Delineating Mechanisms for Knickpoint Development**

As depicted above (Figure 4), knickpoints develop from a number of reasons. The identified knickpoints were overlaid with King's (1948) geologic map of the Southern Guadalupe Mountains, obtained from the US Geological Survey National Geologic Map Database (NGMDB). Erosional features, including knickpoints, associated with geologic contacts, river confluences, or other geologic features such as folds or faults are considered static features of those entities. Features lacking geologic association are commonly assumed to have formed due to other mechanisms including tectonic or climatic influences (Wobus et al., 2006; Ellis et al., 2014), and often mark a divide between actively adjusting, disequilibrium landscapes downstream, and relict landscapes upstream. These particular knickpoints are referred to as migratory knickpoints. While the list of possibilities are extensive, multiple mechanisms of knickpoint development must be considered and evaluated to address driving forces of landscape evolution.

### **Application of Flint's Law**

After knickpoints were identified, Flint's Law was applied to equilibrium reaches of stream channels and was solved using simple regression analyses with codes written in R.  $K_s$  and  $\theta$  values were obtained for each stream segment (Table 1). A regional concavity index was calculated to be  $\theta_{\text{ref}} = 0.469$ , and used in further calculations to estimate  $K_{\text{sn}}$  values across the

Southern Guadalupe Mountains. Residual errors from Flint's Law regression analyses were recorded per river-channel for later use in data analysis.

### **Data Analysis**

Statistical and qualitative analyses were performed to answer the hypotheses: (H<sub>1</sub>) rebound values differ between geologic units, (H<sub>2</sub>) channel gradient and knickpoints are controlled by rock strength (rebound), and (H<sub>3</sub>) residual errors from Flint's Law regression analyses are explained by rebound. Statistical relationships were determined at the reach, stream, canyon, and regional scales with a significance of  $\alpha = 0.05$ . Since the relationships between rebound, stream morphometry, and Flint's Law is relatively unexplored, this study hereby considers anything with an  $\alpha < 0.2$  (>80%) to be significant. To test the first hypothesis, weighted mean rebound and weighted standard deviations were calculated per geologic unit. Overall bedrock mean rebound values that are within one standard deviation from each other are considered statistically similar in terms of rock-strength (Ellis et al., 2014). Conversely, those exceeding one standard deviation of difference are considered statistically different (Ellis et al., 2014). Although lacking empirical evidence, the assumption is that two rocks with similar rebound values should exhibit similar erodibilities. Simple qualitative observation of landscape morphometry at geologic contacts can alleviate uncertainties associated with this assumption. Additional confidence in final weighted rebound values was determined through simple statistical regression analysis using rebound as the independent variable and  $K_{sn}$  as the dependent variable. In this case, rebound (rock strength) should increase with increased  $K_{sn}$  values (Equation 4).

The second hypothesis was tested using simple statistical regression analysis and qualitative observation. Regressions analyses were performed on mean rebound (independent) and slope (dependent) values, and tested for Pearson's correlation coefficient. Data validity was confirmed using the Breusch Pagan test for homoscedasticity, and the Shapiro Wilks test for normality. Qualitative relationships between rebound (rock strength) and knickpoint development evaluated using 2-dimensional graphs constructed in R and maps constructed in ArcMap (v.10).

Simple regression analysis was also performed on mean rebound values (independent) and Flint's Law residual errors (dependent) to test the third and final hypothesis. Since topographic data were resampled to smooth profiles and reduce error, we believe the remaining residual errors will predominately reflect geomorphic features, rather than inherent modeling errors. Similar to the tests performed on the second hypothesis, regression analyses were accompanied by tests for Pearson's correlation coefficient, the Breusch Pagan test for heteroscedasticity, and the Shapiro Wilks test for normality.

TABLE 1		Flint's Law Regression Analysis											
River Name	River	Lower Segment		Middle Segment		Upper Segment		Lower Segment		Middle Segment		Upper Segment	
		Regression Fit	r <sup>2</sup>	Regression Fit	r <sup>2</sup>	Regression Fit	r <sup>2</sup>	Log(Ks)	θ	Log(Ks)	θ	Log(Ks)	θ
PS1	1	y = 1.16 - 0.35x	0.196	-	-	y = -7.78 + 1.13x	0.474	0.35	1.16	-	-	-	-7.78
PS2	2	y = 1.11 - 0.34x	0.230	-	-	y = -4.00 + 0.52x	0.280	0.34	1.11	-	-	-	-4.00
PS3	3	y = -0.33 - 0.13x	0.038	-	-	y = -1.38 + 0.09x	0.003	0.13	-0.33	-	-	-	-1.38
PS4	4	y = 4.16 - 0.79x	0.730	-	-	y = -0.44 + 0.02x	0.035	0.79	4.16	-	-	-	-0.44
MC1	5	y = 4.56 - 0.80x	0.140	y = -8.98 + 1.28x	0.108	y = 0.01 - 0.20x	0.077	0.80	4.56	-	-8.98	0.20	0.01
MC2	6	-	-	-	-	y = 1.62 - 0.46x	0.406	-	-	-	-	0.46	1.62
MC3	7	-	-	-	-	y = 1.09 - 0.38x	0.486	-	-	-	-	0.38	1.09
MC4	8	y = 3.86 - 0.83x	0.152	y = -2.16 + -0.13x	0.007	y = -0.46 - 0.16x	0.229	0.83	3.87	-	-2.16	-	-0.46
MC5	9	y = 3.49 - 0.65x	0.377	y = 2.79 - 0.54x	0.048	y = -1.12 - 0.02x	0.000	0.65	3.49	0.54	2.79	-	-1.12
MC6	10	-	-	-	-	y = 1.89 - 0.53x	0.243	-	-	-	-	0.53	1.89
MC7	11	y = 4.98 - 0.85x	0.163	-	-	y = 1.82 - 0.41x	0.105	0.85	4.98	-	-	0.41	1.82
MC8	12	y = 4.00 - 0.72x	0.422	y = 1.92 - 0.43x	0.336	-	-	0.72	4.00	0.43	1.92	-	-
MC9	13	y = 3.72 - 0.70x	0.507	-	-	y = -3.57 + 0.53x	0.162	0.70	3.72	-	-	-	-3.57
MC10	14	y = 2.59 - 0.54x	0.335	-	-	-	-	0.54	2.59	-	-	-	-
MC11	15	y = 2.54 - 0.56x	0.544	y = -0.36 - 0.10	0.001	-	-	0.56	2.54	0.10	-0.36	-	-
MC12	16	y = -0.89 - 0.09x	0.050	-	-	-	-	0.09	-0.89	-	-	-	-
MC13	17	y = 0.78 - 0.32x	0.230	-	-	-	-	0.32	0.78	-	-	-	-
								avg	2.55	0.36	-1.36	0.39	-1.03
								θ <sub>ref</sub>	0.43				

## CHAPTER IV

### RESULTS

#### **Rebound and Erodibility between Geologic Units**

Schmidt Hammer analysis for King's (1948) individual geologic units shows that rebound values do not significantly differ from the overall mean rebound value of  $62.3 \pm 6.5$  (Table 2; Figure 9). However, discrete differences in weighted rebound values do exist. For example, Capitan-*massive* limestone (ls.) units exhibit rebound values ( $70.5 \pm 2.1$ ) that are statistically larger than Goat Seep ls. ( $66.1 \pm 0.6$ ), Capitan-*brecciated* ls. ( $63.5 \pm 2.6$ ), Cherry Canyon sandstone (Ss.) ( $60.0 \pm 4.6$ ), and Bell Canyon Ss. ( $44.8 \pm 16.1$ ). The greatest rebound value ( $72.3 \pm 2.8$ ) occurred within McKittrick Canyon's Capitan ls., and the smallest recorded ( $30.3 \pm 0.8$ ) within Pine Springs Canyon's Bell Canyon sandstone.

Rock mass strength values (RMS) and normalized steepness indices ( $K_{sn}$ ) are often considered parameters that are capable of estimating erodibility (Selby, 1982; Ellis et al., 2014). Regional weighted rebound values pitted against RMS values show a non-significant relationship ( $p = 0.383$ ) (Table 3). However, there are significant relationships ( $p < 0.05$ ) between weighted rebound and mean  $K_{sn}$  values at the regional scale, in Pine Springs Canyon, and within certain stream channels (Table 4; Figure 9). Channels that display significant relationships between rebound and  $K_{sn}$  are PS1, PS2, PS4, MC5, and MC12, (Table 4). These stream channels are located in relatively simple tectonic and hydrologic regimes. For some statistical analyses, middle and lower segments of streams were disregarded to avoid data redundancies and are therefore, only represented by their upper segments (i.e. MC2, MC3, and MC6). These streams

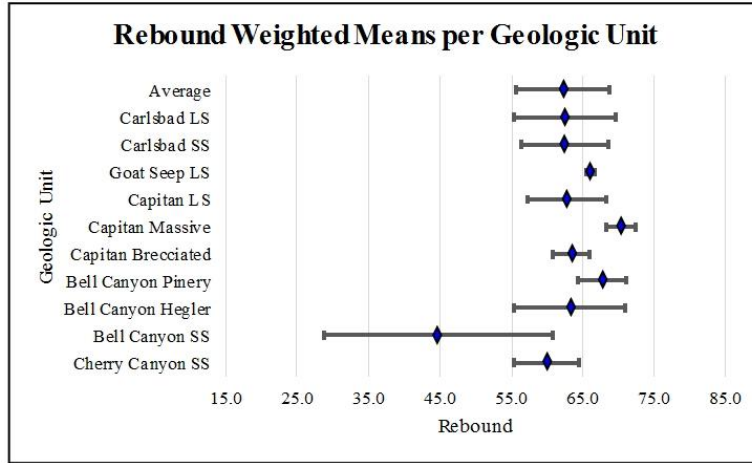


Figure 9: Weighted Mean Rebound per Geologic Unit with Standard Deviations.

TABLE 2 <u>Rebound Weighted Means/STDV</u>			
Geologic Unit	Rebound	SD	n
Cherry Canyon SS	60.0	4.6	20
Bell Canyon SS	44.8	16.1	44
Bell Canyon Hegler	63.1	7.9	121
Bell Canyon Pinery	67.8	3.3	20
Capitan Brecciated	63.5	2.6	80
Capitan Massive	70.5	2.1	20
Capitan LS	62.8	5.7	100
Goat Seep LS	66.1	0.6	40
Carlsbad SS	62.5	6.2	20
Carlsbad LS	62.5	7.2	20
Average	62.3	6.5	

may contain missing values due to insufficient data from the occurrence of two or less geologic units outcropping within their channels.

TABLE 3	Rebound vs RMS Regression Analysis						
	<i>Slope</i>	<i>Intercept</i>	$r^2$	<i>P</i>	<i>BP</i>	<i>Shapiro</i>	<i>r</i>
Regional	0.287	57.564	0.048	0.383	0.406	0.701	0.219

TABLE 4		Rebound vs K <sub>sn</sub> Regression Analysis						
		<i>Slope</i>	<i>Intercept</i>	$r^2$	<i>p</i>	<i>BP</i>	<i>Shapiro</i>	<i>r</i>
	Regional	9.3	-526	0.574	0.029	0.310	0.792	0.758
	PS	11.7	-676	0.598	0.041	0.049	1.000	0.773
	MC	7.4	-420	0.445	0.148	0.674	0.834	0.667
	MCS	9.2	-528	0.357	0.211	0.621	0.698	0.597
	MCN	5.3	-281	0.290	0.350	0.114	0.409	0.538
PS1	River-1	5.1	-268	0.695	0.020	0.792	0.349	0.260
PS2	River-2	4.4	-221	0.709	0.074	0.113	0.651	0.154
PS3	River-3	3.2	-141	0.621	0.113	0.495	0.315	0.069
PS4	River-4	21.9	-1303	0.853	0.077	0.216	0.490	0.698
Mc1	River-5	2.2	-91	0.082	0.582	0.162	0.176	-0.126
Mc2	River-6	1.8	-84	0.579	0.450	0.091	NA	0.238
Mc3	River-7	40.2	-2493	1.000	NA	NA	NA	0.465
Mc4	River-8	2.6	-116	0.117	0.573	0.194	0.723	-0.022
Mc5	River-9	12.0	-712	0.724	0.068	0.153	0.753	0.348
Mc6	River-10	-18.3	1168	1.000	NA	NA	NA	-0.442
Mc7	River-11	3.4	-141	0.083	0.711	0.221	0.898	-0.039
Mc8	River-12	4.5	-216	0.164	0.595	0.228	0.926	0.049
Mc9	River-13	11.1	-631	0.302	0.337	0.351	0.147	0.117
Mc10	River-14	2.2	-52	0.038	0.805	0.273	0.616	0.052
Mc11	River-15	0.6	7	0.007	0.916	0.303	0.832	-0.093
Mc12	River-16	2.8	-143	0.965	0.119	0.093	NA	0.173
Mc13	River-17	7.5	-440	0.985	0.077	0.093	NA	0.110



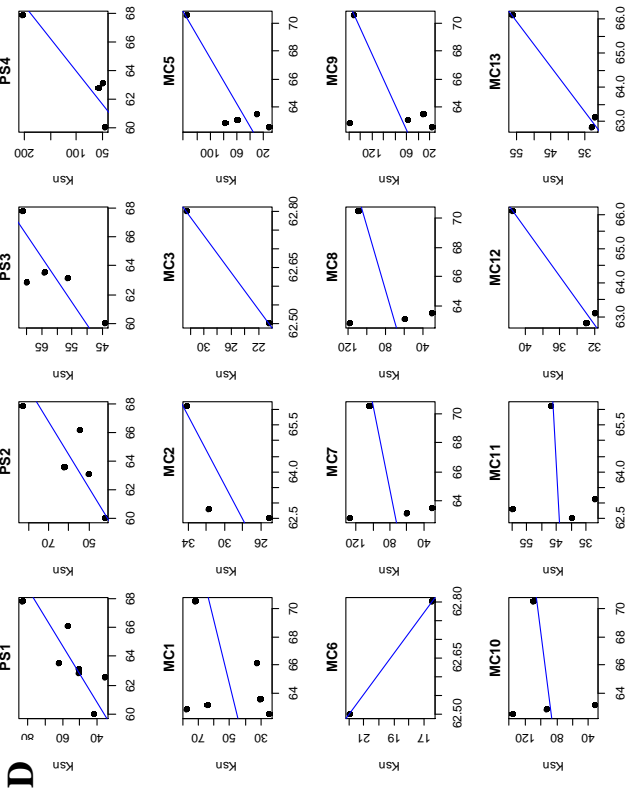
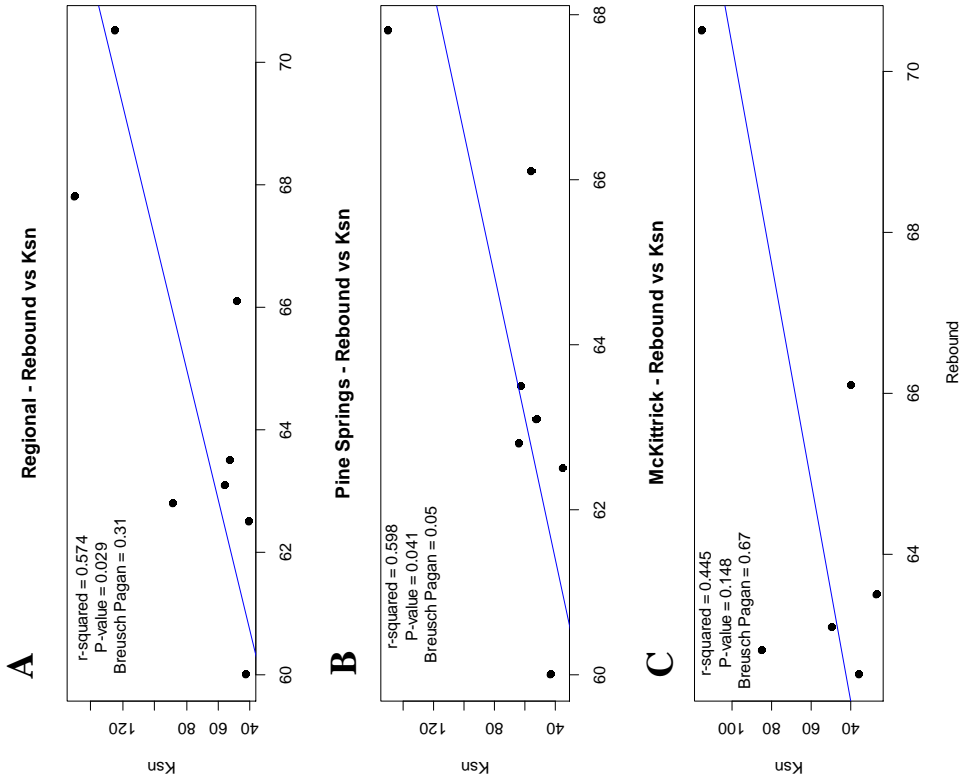


Figure 10: Regression Analyses between Rebound and Normalized Steepness ( $K_{sn}$ ) (A) regionally, in (B) Pine Springs Canyon,, (C) McKittrick Canyon, and (D) individual streams.

### **Relationships between Rebound and Stream Gradient/Knickpoints**

Several slope-break knickpoints exist within the stream profiles of the Southern Guadalupe Mountains in association with various geologic phenomena (Appendix A). For example, knickpoints in Pine Springs Canyon and Southern McKittrick Canyon occur near major stream confluences, and in Northern McKittrick Canyon where there is a geologic contact between Capitan ls. ( $R = 62.8 \pm 5.7$ ) and Goat Seep ls. ( $R = 66.1 \pm 0.6$ ) (Figure 8). There are also instances in Southern McKittrick Canyon where knickpoints coincide with major northwest-southeast trending normal faults that appear to separate a lower, convex profile downstream from smooth concave profiles upstream (Figure 15). While most knickpoints appear to have strong qualitative geologic associations, one knickpoint exists within MC10 without any geologic or hydrologic association (Figure 14).

Mean rebound and mean  $K_{sn}$  values tend to change on either side of the identified knickpoints, and generally increase in the upstream direction. Specifically, at the regional scale, mean rebound and  $K_{sn}$  values are lowest in downstream segments ( $\bar{R}_L = 63.8$ ;  $\bar{K}_{snL} = 76.3$ ), highest in middle segments ( $\bar{R}_M = 65.0$ ;  $\bar{K}_{snM} = 92.0$ ), and moderate in upper segments ( $\bar{R}_U = 64.5$ ;  $\bar{K}_{snU} = 79.1$ ).

There is a strongly positive, significant relationship between weighted mean rebound and stream gradient (or slope) at the regional scale ( $r^2 = 0.563$ ;  $p = 0.039$ ;  $r = 0.751$ ) (Table 5; Figure 11). There is also a significantly weak to moderately strong positive relationship at the tributary scale ( $r = 0.392 - 0.502$ ) for tributaries PS1 ( $r^2 = 0.686$ ;  $p = 0.021$ ), PS4 ( $r^2 = 0.902$ ,  $p = 0.050$ ), MC5 ( $r^2 = 0.805$ ;  $p = 0.039$ ) PS2 ( $r^2 = 0.751$ ;  $p = 0.057$ ), and MC8 ( $r^2 = 0.815$ ;  $p = 0.097$ ). The aforementioned rivers exist within relatively simple tectonic and hydrologic regimes. Tributaries

that cross both confluence and tectonic knickpoints, such as MC1 and MC4, have no correlation between rebound and stream gradient ( $p > 0.1$ ).

<u>TABLE 5</u>		<u>Rebound vs Stream Gradient Regression Analysis</u>						
		<i>Slope</i>	<i>Intercept</i>	$r^2$	$p$	<i>BP</i>	<i>Shapiro</i>	$r$
Regional		0.032	-1.9	0.563	0.032	0.178	0.330	0.751
PS		0.041	-2.5	0.562	0.052	0.028	0.852	0.750
MC		0.028	-1.7	0.649	0.053	0.998	0.655	0.806
MCS		0.032	-2.0	0.706	0.036	0.953	0.992	0.840
MCN		0.010	-0.5	0.133	0.546	0.094	0.629	0.365
PS1	River-1	0.007	-0.4	0.686	0.021	0.160	0.740	0.392
PS2	River-2	0.008	-0.4	0.751	0.057	0.157	0.582	0.389
PS3	River-3	0.004	-0.1	0.045	0.732	0.540	0.191	-0.119
PS4	River-4	0.089	-5.4	0.902	0.050	0.779	0.021	0.694
Mc1	River-5	0.000	0.0	0.003	0.916	0.476	0.580	-0.032
Mc2	River-6	0.010	-0.6	0.905	0.200	0.091	NA	0.539
Mc3	River-7	0.101	-6.3	1.000	NA	NA	NA	0.502
Mc4	River-8	0.000	0.0	0.000	0.977	0.330	0.883	-0.068
Mc5	River-9	0.017	-1.0	0.805	0.039	0.407	0.596	0.502
Mc6	River-10	-0.047	3.0	1.000	NA	NA	NA	-0.484
Mc7	River-11	0.039	-2.4	0.674	0.179	0.201	0.653	0.413
Mc8	River-12	0.027	-1.6	0.815	0.097	0.223	0.909	0.495
Mc9	River-13	0.035	-2.1	0.307	0.332	0.385	0.196	0.157
Mc10	River-14	0.004	-0.1	0.021	0.856	0.254	0.832	0.077
Mc11	River-15	-0.004	0.4	0.032	0.821	0.436	0.297	-0.166
Mc12	River-16	0.012	-0.7	0.902	0.203	0.093	NA	0.478
Mc13	River-17	0.018	-1.1	0.942	0.155	0.093	NA	0.185

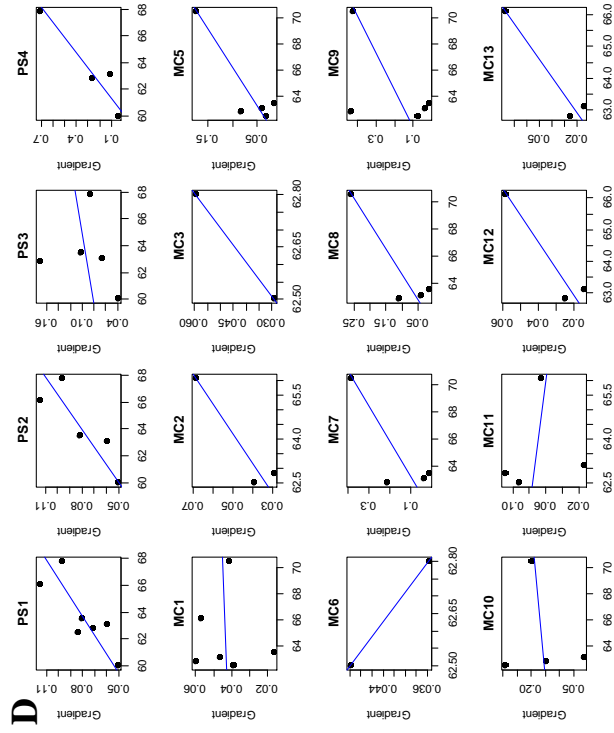
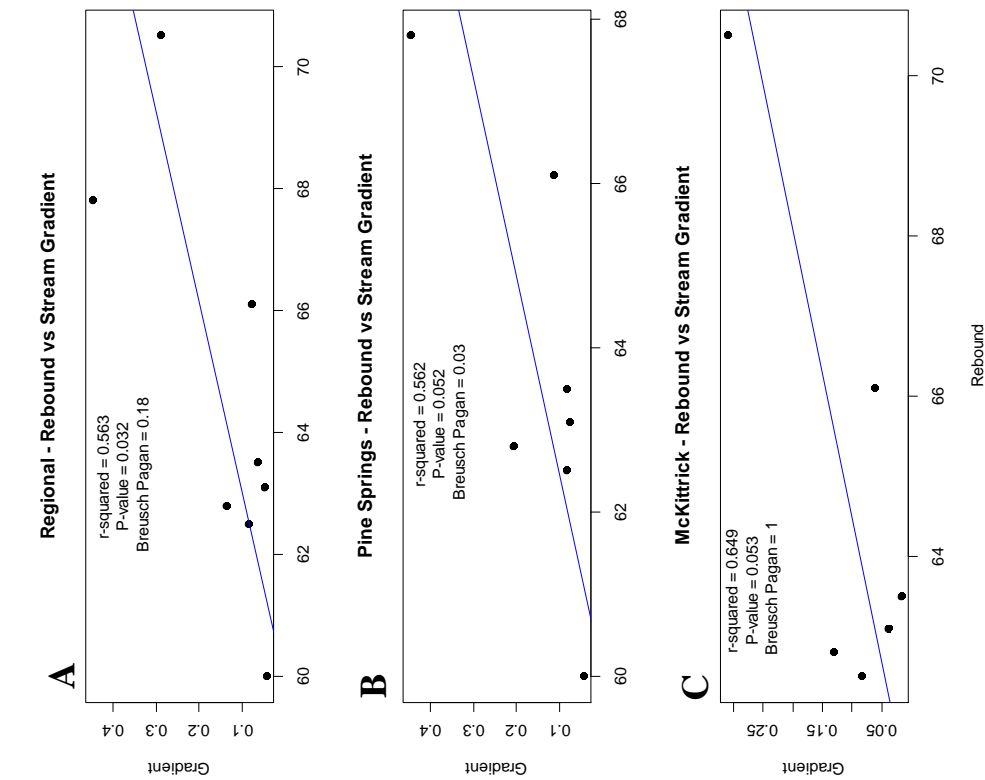


Figure 11: Regression Analyses between Rebound and Channel Gradient (Slope) (A) regionally, in (B) Pine Springs Canyon, (C) McKittrick Canyon, and (D) individual streams.

### **Relationships between Rebound and Flint's Law Residual Errors**

The residual errors associated with Flint's Law are derived from, per-stream,  $\log(\text{Slope})$ - $\log(\text{Area})$  regression analyses and are referred to herein as residuals, or residual errors. At the regional scale, the relationship between weighted rebound values and residual error is significant ( $r = 0.705$ ;  $p = 0.051$ ) (Table 6) (Figure 12). Similar statistical analysis at the canyon scale show a significant relationship in Pine Springs Canyon, ( $p = 0.011$ ;  $r = 0.867$ ). Additionally, significant yet weaker positively correlated relationships exist at the tributary scale within PS1 ( $r = 0.3$ ;  $p = 0.031$ ), PS2 ( $r = 0.176$ ;  $p = 0.047$ ), and PS3 ( $r = 0.225$ ;  $p = 0.023$ ). Pine Springs Canyon and the aforementioned tributaries are located within relatively simple tectonic and hydrologic regimes. Conversely, tributaries within tectonically and hydrologically complex regimes, including MC1 and MC4, display insignificant relationships and very weak correlations ( $p > 0.05$ ,  $r < |0.06|$ ).

TABLE 6		Rebound vs Residuals Regression Analysis						
		<i>Slope</i>	<i>Intercept</i>	$r^2$	$p$	$BP$	<i>Shapiro</i>	$r$
	Regional	0.019	-1.2	0.497	0.051	0.122	0.449	0.705
	PS	0.030	-1.9	0.752	0.011	0.076	0.390	0.867
	MC	0.018	-1.3	0.193	0.384	0.450	0.211	0.439
	MCS	0.019	-1.3	0.197	0.377	0.455	0.223	0.444
	MCN	0.017	-1.1	0.317	0.323	0.140	0.426	0.563
PS1	River-1	0.038	-2.4	0.637	0.031	0.674	0.097	0.300
PS2	River-2	0.031	-2.0	0.780	0.047	0.158	0.523	0.176
PS3	River-3	0.034	-2.1	0.861	0.023	0.548	0.399	0.225
PS4	River-4	0.026	-1.6	0.159	0.601	0.727	0.213	0.473
Mc1	River-5	-0.004	0.1	0.004	0.906	0.556	0.044	-0.047
Mc2	River-6	0.017	-1.1	0.372	0.583	0.091	NA	0.155
Mc3	River-7	0.684	-42.9	1.000	NA	NA	NA	0.567
Mc4	River-8	0.010	-0.7	0.046	0.728	0.380	0.475	-0.053
Mc5	River-9	0.023	-1.5	0.211	0.437	0.464	0.317	0.203
Mc6	River-10	0.011	-0.6	1.000	NA	NA	NA	0.006
Mc7	River-11	0.019	-1.2	0.574	0.242	0.292	0.584	0.104
Mc8	River-12	0.019	-1.4	0.161	0.599	0.271	0.789	0.070
Mc9	River-13	0.023	-1.6	0.138	0.538	0.184	0.948	-0.004
Mc10	River-14	0.011	-0.8	0.157	0.603	0.319	0.243	0.037
Mc11	River-15	-0.007	0.5	0.298	0.454	0.220	0.621	-0.070
Mc12	River-16	0.084	-5.6	0.392	0.569	0.093	NA	0.173
Mc13	River-17	0.038	-2.5	0.529	0.482	0.093	NA	0.132

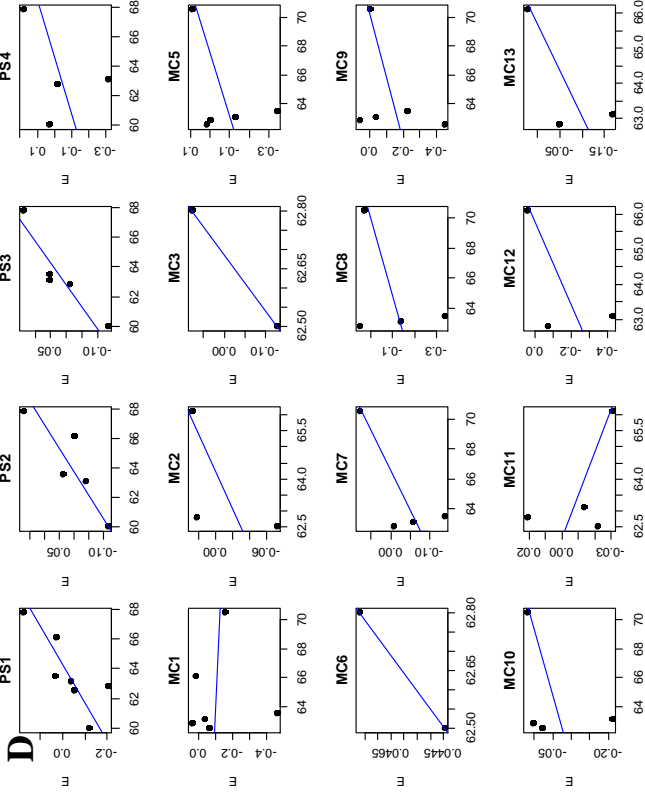
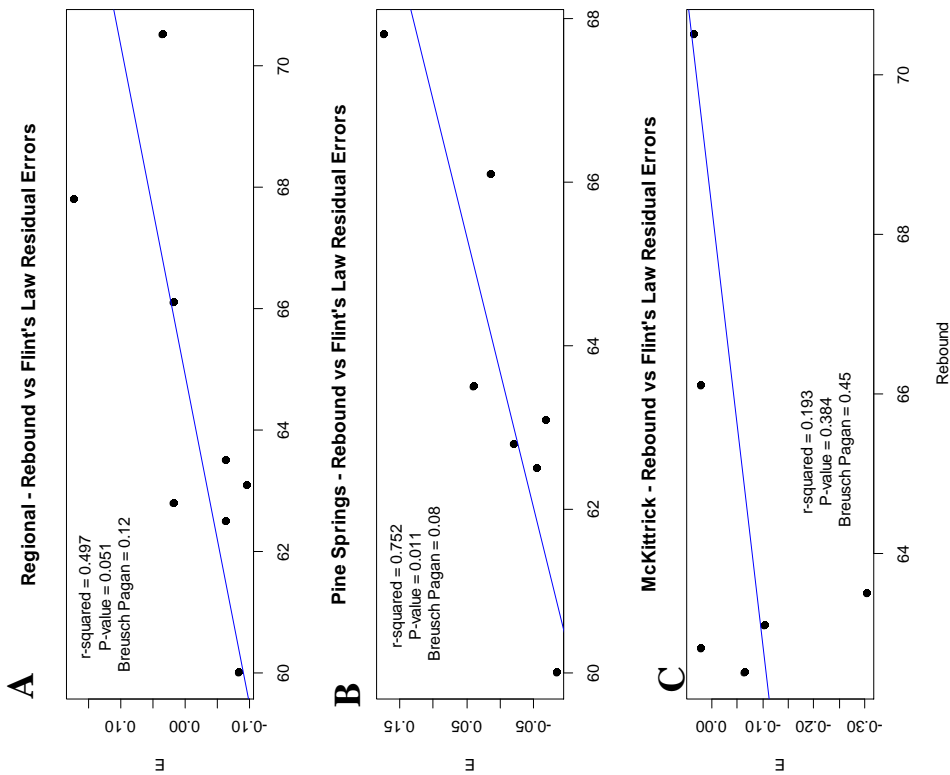


Figure 12: Regression Analyses between Rebound and Flint's Law Residual Errors (A) regionally, in (B) Pine Springs Canyon, (C) McKittrick Canyon, and (D) individual streams.

## CHAPTER V

### DISCUSSION

#### **Rebound and Erodibility**

Schmidt hammer analysis supports our first hypothesis, suggesting that rebound values do indeed differ between King's (1948) geologic units with the Capitan-*massive* ls. displaying the highest weighted rebound value of  $70.5 \pm 2.1$ . However, refuting our first hypothesis, the majority of geologic units have similar weighted mean rebound measurements, averaging  $62.3 \pm 6.5$  (Figure 9). While the overarching assumption with Schmidt hammer analysis is that a single weighted mean rebound value represents one geologic unit, this may not be the case. Longitudinal profiles reveal that contacts between two geologic units with similar hardnesses can still exhibit differential erodibility. Additionally, local variations in rebound that exceed one standard deviation of difference could exist within one lithology and thus cause localized variations in erodibility. Therefore, significant local variations in rebound could alter any conclusions drawn from this analysis.

Rebound alone may not indicate erodibility. Therefore, a comparison must be drawn between rebound and other measurements of erosional competency including RMS and normalized steepness ( $K_{sn}$ ) values. Statistical analysis between weighted mean rebound and RMS values suggests no correlation between rebound and erodibility in the Southern Guadalupe Mountains. This finding could be due to low RMS data resolution, unidentified errors in data collection, or because rebound values, indeed, do not scale with erodibility.

Utilizing  $K_{sn}$ , we can make assumptions to infer erosional efficiency (Equation 4). Assuming relatively uniform uplift rates across the Southern Guadalupe Mountains;  $K_{sn}$  values



should correlate negatively with erodibility (Equation 4). Thus, if erodibility decreases with increasing rebound values,  $K_{sn}$  will share an indirect positive relationship with rebound. In this case, the statistical relationship between  $K_{sn}$  and rebound is significantly positively correlated at the regional, canyon, and stream scales. Therefore, we suggest that despite null relationships between rebound and RMS, rebound values can be used to predict the relative erodibility of geologic units in the Southern Guadalupe Mountains. However, the relationship between rebound and  $K_{sn}$  is more complex at smaller scales.

While  $K_{sn}$  and rebound share a significantly positive relationship across the region as well as in Pine Springs Canyon, no such relationships exist within McKittrick canyon. This disparity in statistical analysis could occur for several reasons: 1) upstream drainage area (i.e. stream capture) and local faulting could more significantly affect bedrock erosion and slope development; 2) a lack of data resolution from limited bedrock exposures within stream channels (i.e. channels in northern McKittrick Canyon); 3) rebound values are not positively correlated with erodibility; or 4) uplift rates are not uniform across the Southern Guadalupe Mountains.

Due to the presence of complex hydrologic and tectonic regimes in McKittrick Canyon, and rebound-data limitations within channels such as MC10, 11, 12, and 13, the first and second scenarios are most likely. Thus, the relative erodibility of geologic units can be predicted from rebound values under the circumstances that 1) there is significant data resolution in terms of rebound, and 2) stream channels display relatively simple tectonic and hydrologic regimes.

## **Stream Gradient and Knickpoint Development**

Stream gradient (slope) is strongly positively correlated with rebound in the Southern Guadalupe Mountains. However, this relationship is strongest at the channel-scale in channels with relatively simple tectonic and hydrologic regimes and weakest, or nonexistent, in tectonically/hydrologically complex stream channels. This suggests that while stream gradient is strongly dependent on rock strength under simple tectonic/hydrologic regimes, other factors including large increases in drainage area, faulting, and topographic disequilibrium could result in null statistical correlations (Lifton et al., 2009). Qualitatively, the relationships between rock strength and slope are clear in tributaries to major channels such as PS4 and MC5 (Figure 13). This strongly supports our second hypothesis that stream gradient is indeed dependent on rock strength in this region, and suggests a strong likelihood that knickpoints will develop at geologic contacts despite having statistically similar rebound values.

Knickpoints within the Southern Guadalupe Mountains often separate channels into upper, lower, and sometimes middle segments. Several knickpoints exist due to clear lithologic, fault, and confluence associations (Appendix A). However, one knickpoint exists within MC10 without any geologic or hydrologic association (Figure 14). This may be due to the occurrence of unidentified geologic contacts, or complex processes including migratory knickpoint development (Wobus et al., 2006; Ellis et al., 2014). If migratory knickpoints are present, then it is possible that others exist within the Southern Guadalupe Mountains, but remain either unidentified or muffled by other knickpoints.

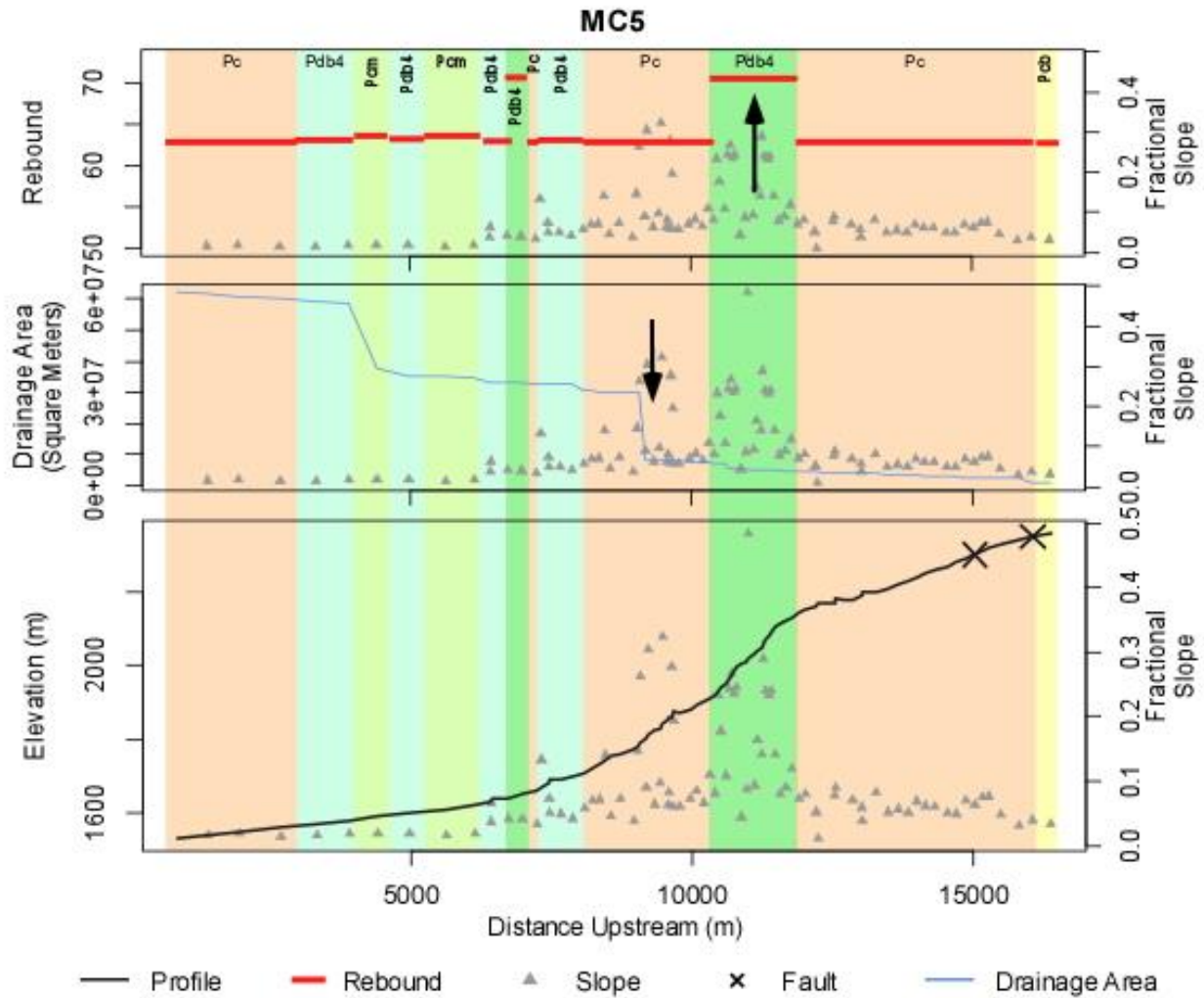


Figure 13: MC5 Longitudinal Stream Profile. This figure shows strong positive relationships between increased rock strength and stream gradient. Notice slope increases in association with increased rebound values and sharp increases in drainage area (black arrows). See Appendix B for geologic symbols key.

While one would assume that lithologic knickpoints should occur at geologic contacts that mark a significant change in rebound values, this is not the case. Pine Springs Canyon's PS1 longitudinal profile contains a lithologic knickpoint at the contact between Bell Canyon Pinery (*Pdb5*) ( $R=67.8\pm3.3$ ) downstream, and Capitan-brecciated ls. (*Pcbr*) ( $63.5\pm2.6$ ), upstream, with

*Pdb5* acting as the cliff-former (Figure 15). Similarly, McKittrick Canyon's MC5 longitudinal profile contains a knickpoint at the contact between Capitan-massive ls. (*Pcm*)(70.5±2.1) downstream, and Capitan ls. (*Pc*)(62.8) upstream, where *Pcm* is the cliff-former (Figure). This is also the case in the longitudinal profile of MC11 where Goat Seep (66.1±0.6)(*Pg*), contacts *Pc* (62.8±5.7). These observations further support the second hypothesis that harder bedrock acts as the slope former, and suggests that knickpoints can still develop at a lithologic contact where geologic units contain significantly-similar rebound values. Therefore, based on similar strength rocks (rebound) having different erosion potentials (Figure10), lumping different lithologies together based on similar rebound values is an overgeneralization and should be avoided.

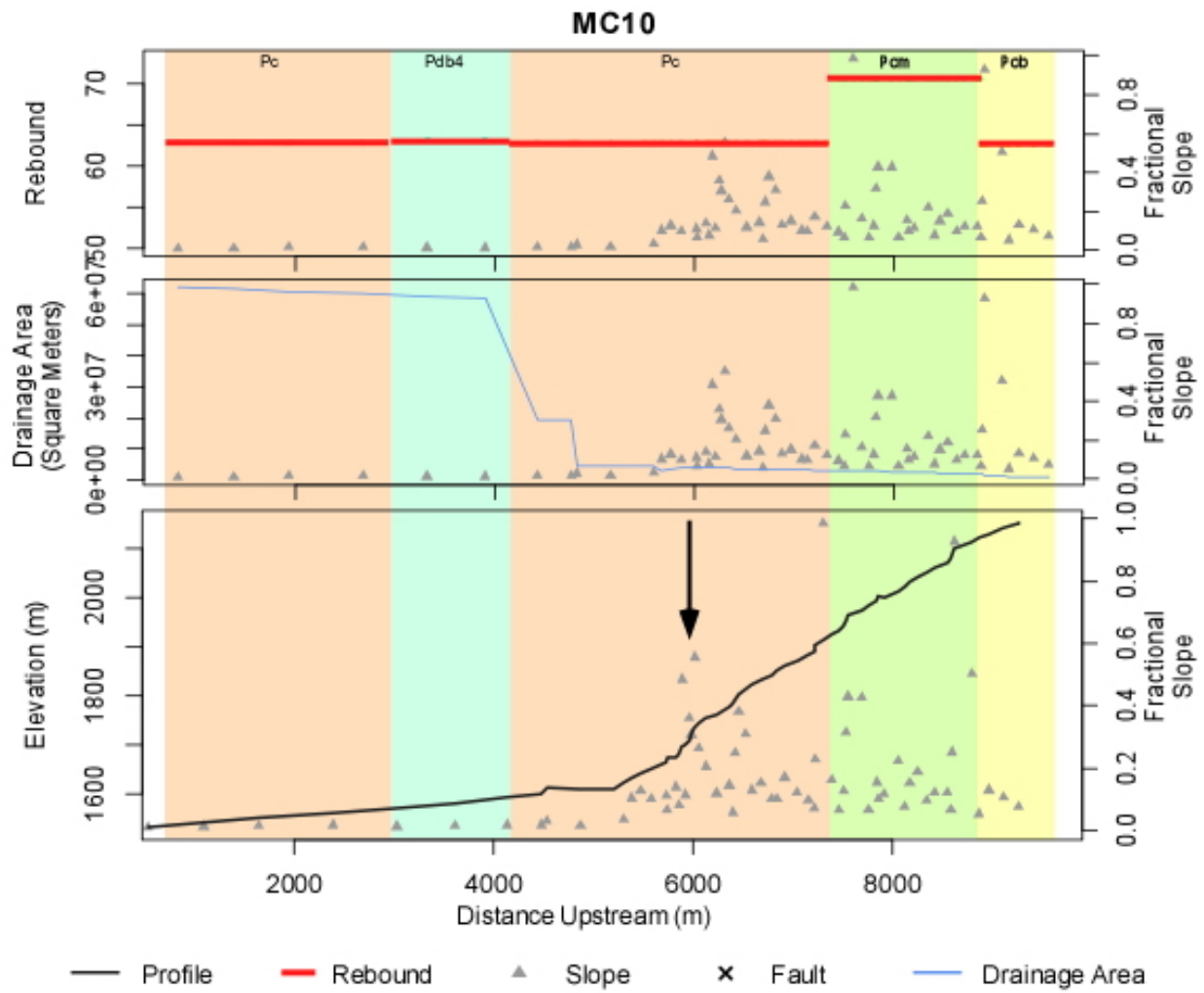


Figure 14: MC10 Longitudinal Stream Profile. This figure displays a knickpoint with no geologic or hydrologic association (black arrow). See Appendix B for geologic symbols key.

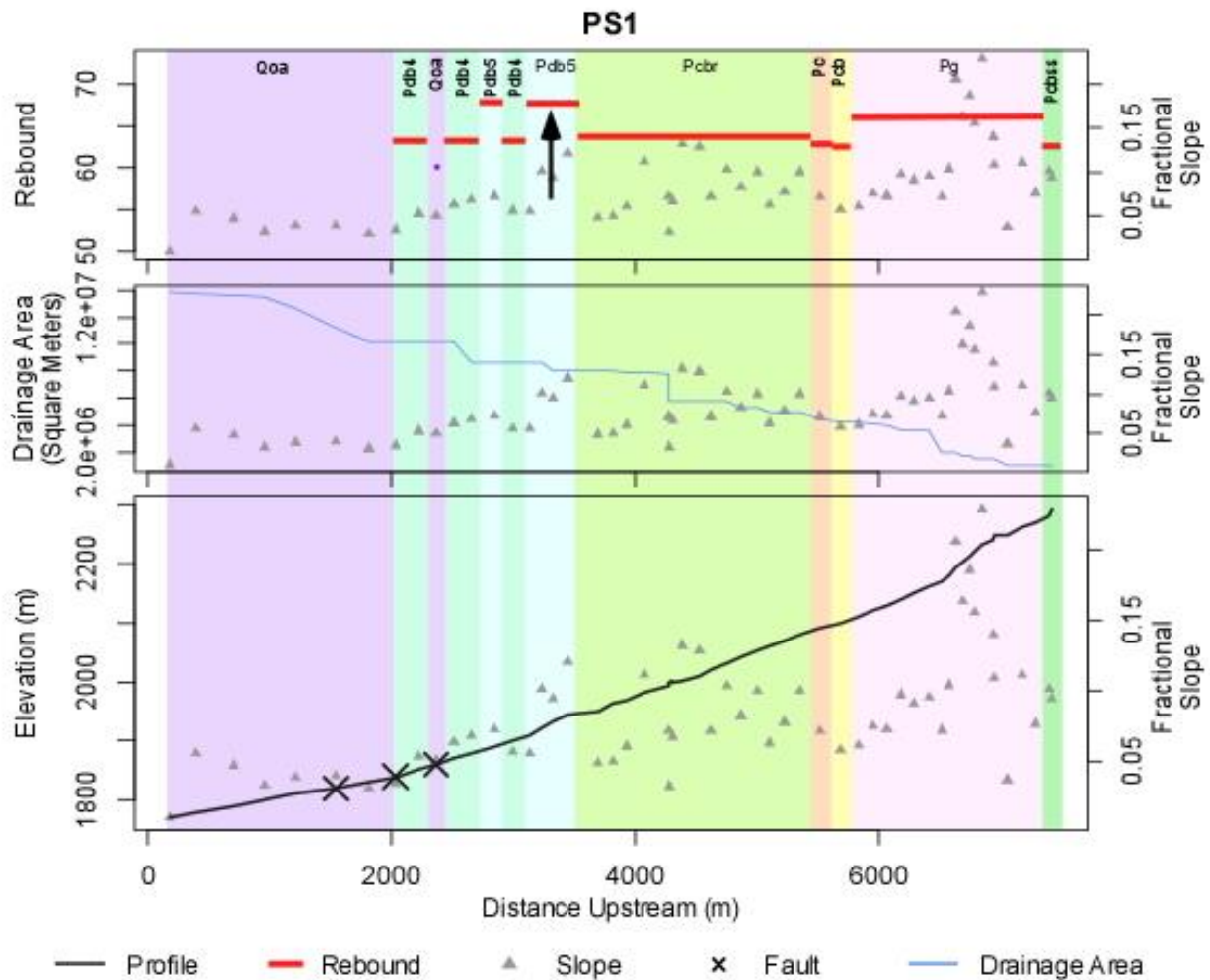


Figure 15: PS1 Longitudinal Stream Profile. This figure displays minor knickpoint development at the contact of Pdb5 (Pinery) and Pcb (Capitan-brecciated) (black arrow). See Appendix B for geologic symbols key.

In an interesting case, faulting within McKittrick Canyon has caused a unique scenario where a knickpoint disrupts the longitudinal profiles of MC1,2,3,4, and 6. The longitudinal stream profile of MC1 clearly shows the relationship between this knickpoint and other environmental conditions (Figure 16). This knickpoint separates an ideal, concave, longitudinal profile upstream, from a convex profile downstream (Figure 17A). The reason for this particular

scenario is likely due to steep normal faulting, and subsequent down-dropping, of the footwall upstream of this knickpoint. Here, the upstream profile has potentially graded to a local pseudo-base level that formed by dam-like processes near or on the fault (Figure 17B). However, field observation is needed to identify the legitimacy of this claim. Supporting this claim however, is the hillslope morphology of the landscape. Average hillslopes and  $K_{sn}$  values are relatively lower upstream of this fault-related knickpoint and relatively higher downstream (Figure 18). Downstream of this knickpoint, hillslopes average 31-degrees, and  $K_{sn}$  values suddenly increase. These values suggest that hillslope processes might dominate sediment transport processes. However, it could also indicate relatively higher uplift rates in the downstream direction.

Each of these possibilities is consistent with the pattern of normal faulting where stream power would decrease at the mid-profile base level, and the channels located in the downstream footwall should display a relative increase in uplift when compared to the hanging wall (Snyder et al., 2000; Kirby and Whipple, 2001). In this scenario, antecedent topographies may have dictated channel placement leading to over-steepened valleys on the footwall as lower segments adjust toward equilibrium.

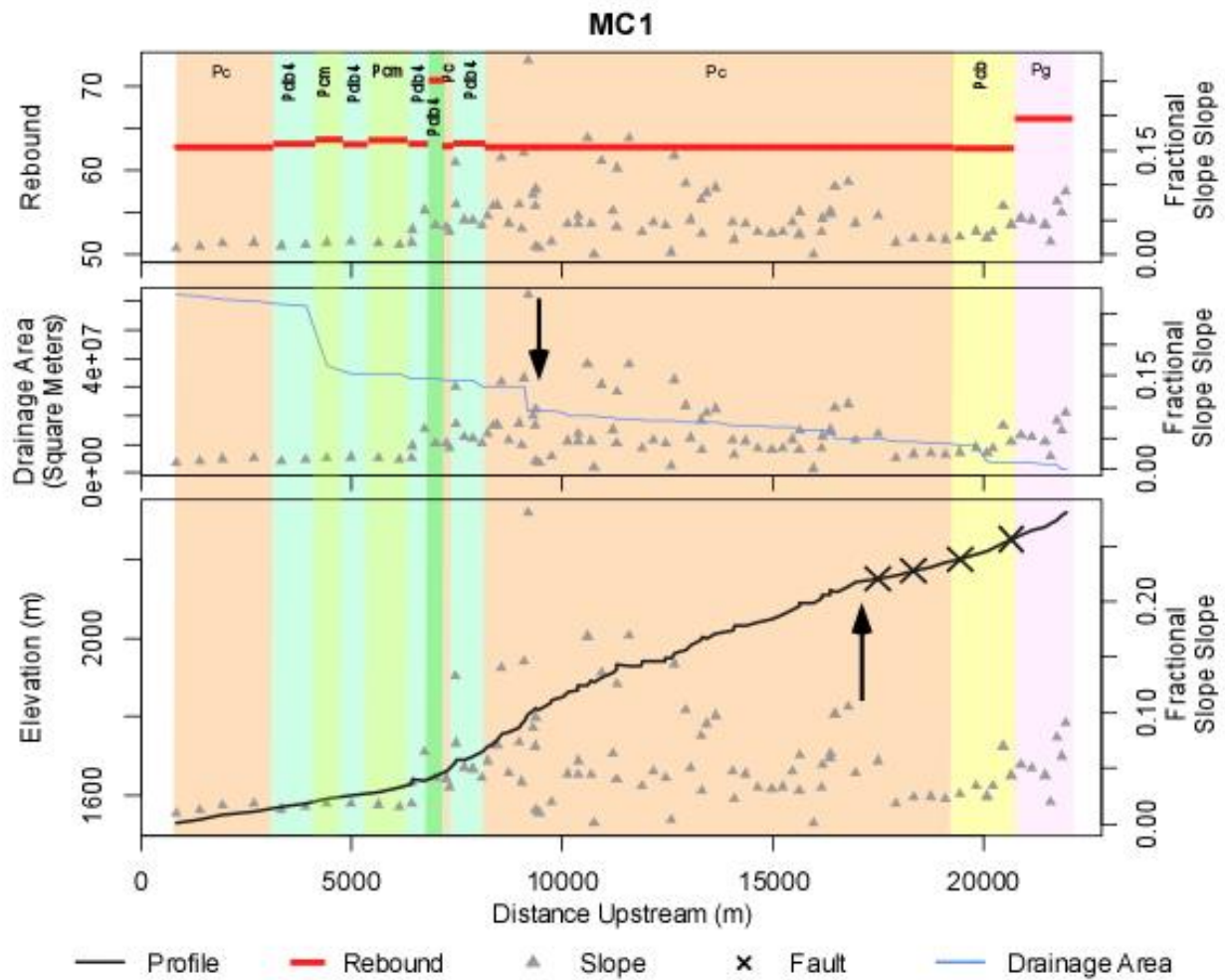


Figure 16: MC1 Longitudinal Stream Profile. This figure displays knickpoints in association with faulting, and sharp increases in drainage area. See Appendix B for geologic symbols key.



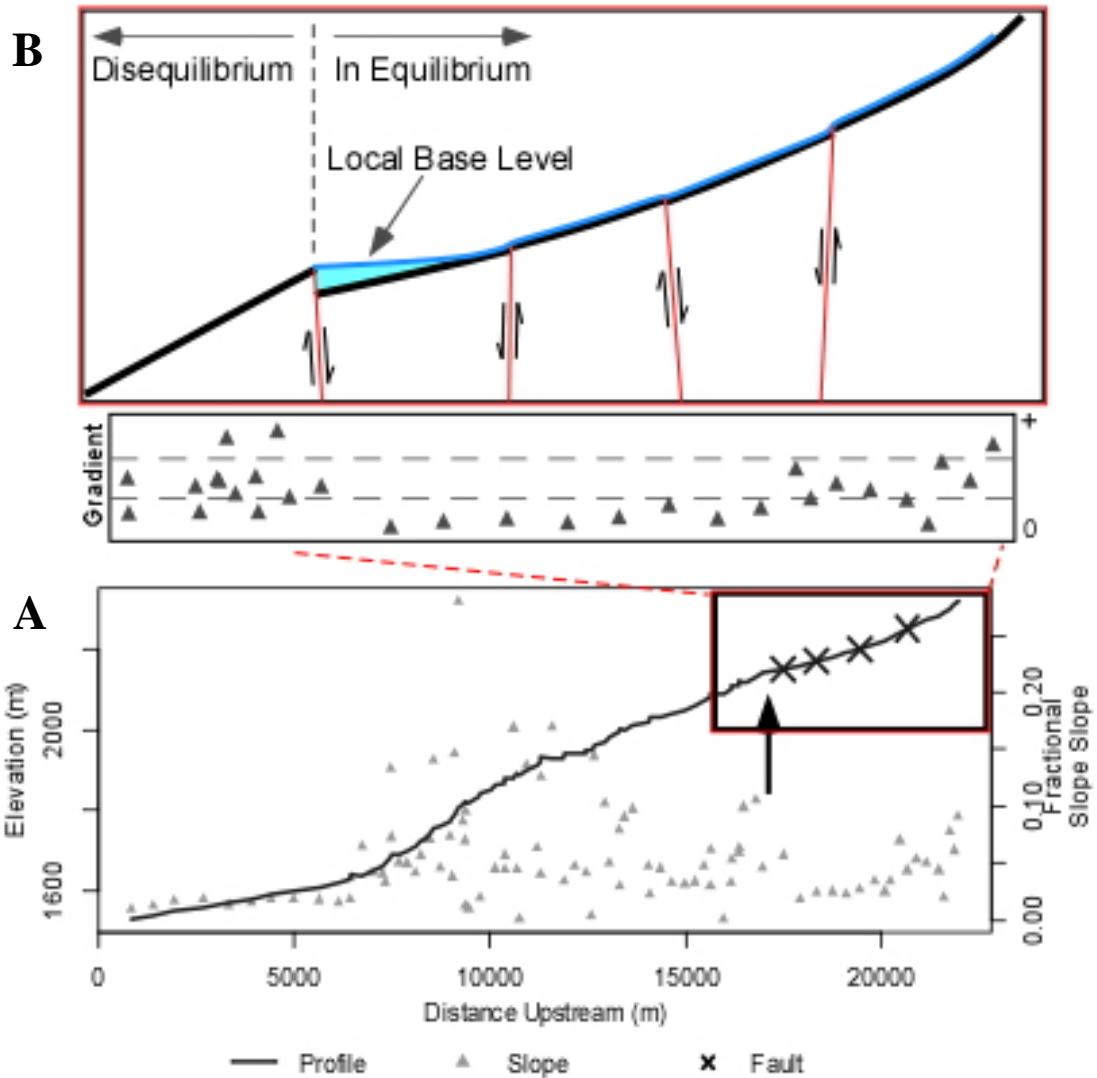


Figure 17: MC1 Stream Profile Interpretation from Faulting. (A) Longitudinal stream profile of MC1 showing a convex middle segment and a concave upper segment separated by steep normal faults. Notice increased stream gradient (fractional slope) in association with faulting. (B) Inset of the upper segment of MC1's longitudinal stream showing the nature of normal faulting, stream gradient, and potential dam-like-structures responsible for the onset of mid-profile base-level.

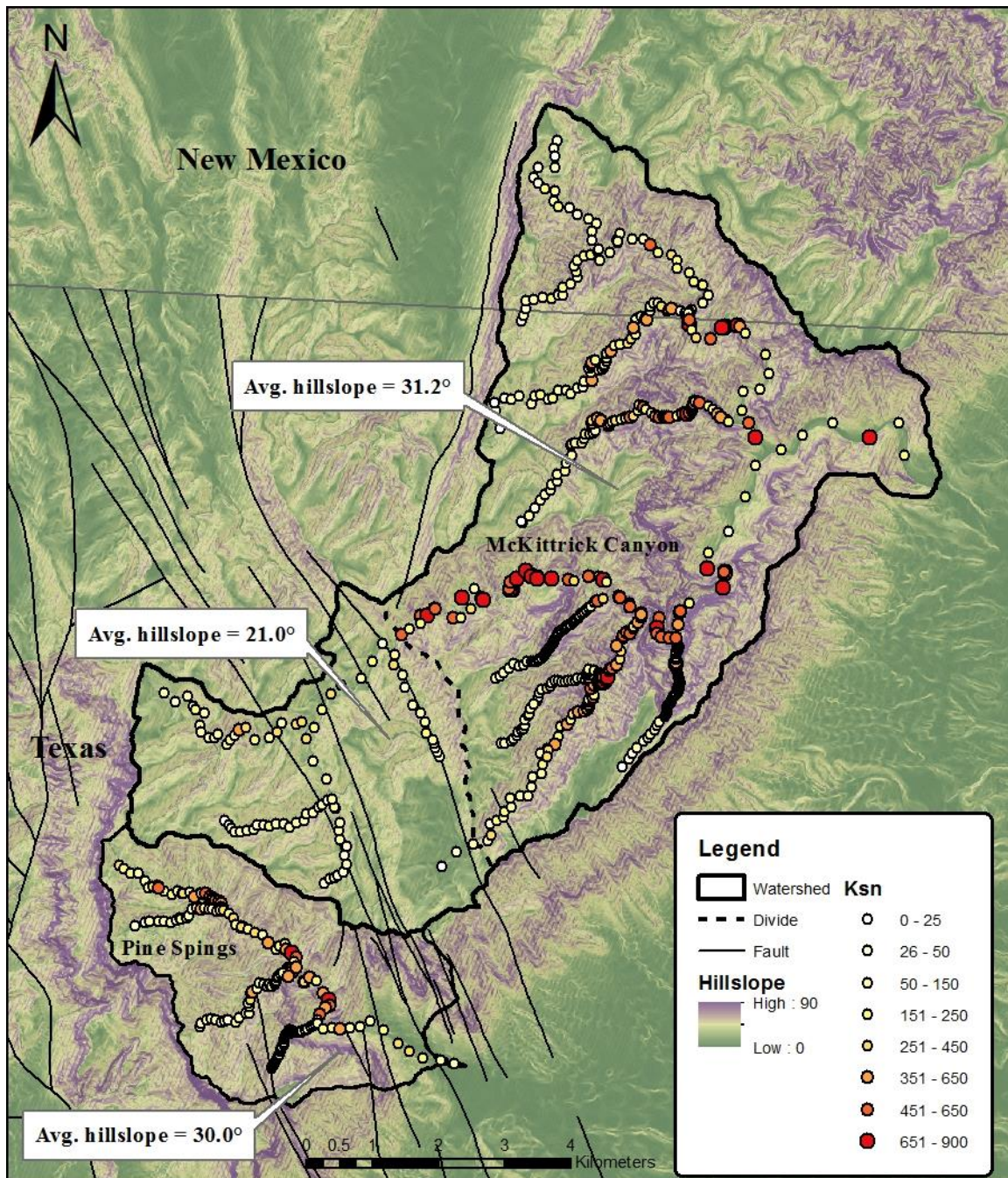


Figure 18: Map of Study Area with the Distribution of Hillslope and Normalized Steepness. Note the distribution of landforms with respect to faulting and the division of high elevation/low relief landscapes upstream from high relief landscapes downstream.

### Flint's Law Residual Errors

Statistical analysis between rebound and residual errors suggests rebound is correlated with the residual errors associated with Flint's Law regression analysis in relatively simple tectonic and hydrologic regimes such as those in Pine Springs Canyon (avg.  $r^2 = 0.759$ , avg.  $r = 0.234$ ,  $p < 0.05$ ). This supports our third hypothesis, however, there is more to the story. While these relationships are apparent in Pine Springs Canyon, these relationships do not exist in tectonically and hydrologically complex regimes found in McKittrick Canyon. This may be due to the nature of complex profiles that intersect major channel confluences (Figure 16) and normal faults (Figure 16, and 17B; Appendix A). Therefore, we suggest that other environmental forces including stream confluences and faulting more greatly affect longitudinal stream morphometry, as compared to rock strength. Some speculation could also be given to the earlier mentioned concept of karst influence (Figure 5), since field observation revealed local changes in the occurrence of flowing water throughout the canyons. Karst swallets and springs may also influence the accuracy of Flint's Law. Finally, these conditions, in concordance with other inherent errors from DEM-processing (Wobus et al., 2006) could help explain why the remaining residual errors are left unpredictable.

Under simple hydrologic/tectonic regimes, there is significant evidence to assume strong correlation between rebound and Flint's Law residual errors. Moreover, referring back to the aforementioned relationships between rebound, rock strength, and stream gradient, an overarching picture begins to develop. We see a strong correlation between rebound and  $K_{sn}$ , which suggests rebound increases as erodibility decreases. This decreased erodibility is strongly positively correlated to increased stream gradient and positively-skewed residual errors. Therefore, rock strength causes over-steepened stream gradients and directly and negatively

affects the accuracy of Flint's Law. While the utilization of this concept to increase the accuracy of Flint's Law is outside the scope of this paper, we can simply assume that Flint's Law residual errors increase as bedrock strength increases, and erodibility decreases. However, and as mentioned several times above, this holds true mostly for hydrologically and tectonically simple catchments. Therefore, as the need for more accurate landscape evolution models increases, the effects from rock strength should be considered as a significant force most influential and predictable in hydrologically and tectonically simple catchments.

### **Future Improvements and Sources of Uncertainty**

Greater data resolution would provide invaluable information related to rebound, RMS,  $K_{sn}$ , knickpoint, and Flint's Law analyses. In the case of Schmidt Hammer analysis, rebound values could be obtained for higher elevation reaches in southern McKittrick Canyon by exploiting various means of canyon access. Field efforts related to this goal were thwarted by large, impassable, boulder deposits and slot canyons. Approaching MC1 from alternative back-country backpacking trails would allow field observations to be made for both rock strength analyses, and confirmation of prior claims pertaining to dam-like structure knickpoints. Data limitations while using rebound as a variable stems from averaging rebound values for one rock type. This can result in statistical tests utilizing only one or two values for regression, and simply output low quality results. Therefore, discreet rebound values might offer more information for mechanical-stratigraphic layers as well as increase statistical resolution.

Another way data quality could be improved upon would be through the use of higher resolution DEMs (<10m). With such resources, we could potentially identify sub-tributary, or reach scale, correlations between rebound and longitudinal morphometry in rivers like MC1,

where both concave and convex longitudinal profiles are present in concordance with knickpoint development. It is also worth mentioning that flowing water was observed in several discreet, but not consistent, locations within the canyons. Areas where the stream reappeared were commonly associated with “bone-marrow-like” tufa deposits. Their locations were not recorded, however future studies could examine the spatial patterns of stream appearance and channel morphometry.

## CHAPTER VI

### CONCLUSION

Seventeen longitudinal stream profiles and twenty-four rock strength measurement sites were chosen for geomorphic assessment in the Southern Guadalupe Mountains, Texas. The primary goals of this paper were to: (1) reveal the variability of rebound and rock strength in the Southern Guadalupe Mountains; (2) identify the relationship between rebound and stream gradient or knickpoint development; and (3) identify any relationships between Flint's Law residual errors and rock strength and erodibility. While the overall rebound value across King's (1948) different geologic units were statistically similar, with Capitan-massive limestone displaying the highest recorded values, these similarities did not indicate similar erosion potential across each unit. In fact, several knickpoints are located at geologic contacts where rebound values are statistically similar. Regression analysis between rebound and RMS reveals no significant relationship. However, other regression analyses suggest significantly strong positive correlations between rebound, erodibility and stream gradient across the Southern Guadalupe Mountains. Interestingly, these relationships are strongest in areas with hydrologically and tectonically simple regimes, suggesting that other processes including increased stream power at river confluences and normal faulting are more strongly affecting landscape evolution in McKittrick Canyon.

Statistical analysis between rebound and residual errors from Flint's Law analysis suggests that errors become more positive with increased slope and increased rebound values. This indirectly assumes that these residual errors can help qualitatively estimate relative erodibilities of exposed bedrock. These methods could likely be used in other study sites in

efforts to uncover similar answers, or help increase the accuracy of landscape evolution models. However, since rebound values can change rapidly over short distances, even within one geologic unit, we suggest using localized rebound values to enhance data resolution. Overall, statistical analysis suggests that rock strength exerts greater influence with more predictable effects on hydrologically and tectonically simple catchments as compared to more complex catchments.

Topographic analysis of this region has also resulted in an interesting discovery within southern McKittrick Canyon. Stream profiles that cross major normal faults reveal equilibrium profiles upstream of faults with convex disequilibrium profiles downstream. One likely cause of this is development of mid-profile base-levels. Upper segments then equilibrate to this pseudo-base-level. Antecedent drainage patterns on the downstream side of this pseudo-base-level may have been set in place long before as the footwall experienced relative uplift. The result is steep hillslopes and channel gradients as the topography strives to attain topographic equilibrium.

## REFERENCES

- Allen, G. H., Barnes, J. B., Pavelsky, T. M., and Kirby, E., 2013, Lithologic and tectonic controls on bedrock channel form at the northwest Himalayan front: *Journal of Geophysical Research: Earth Surface*, v. 118, no. 3, p. 1806-1825, DOI: 10.1002/jgrf.20113.
- Anders, A. M., Roe, G. H., Montgomery, D. R., and Hallet, B., 2008, Influence of precipitation phase on the form of mountain ranges: *Geology*, v. 36, n. 6, p. 479-482, DOI: 10.1130/G24821.
- Basu, A., Aydin, A. 2004, A method for normalization of Schmidt hammer rebound values: *International Journal of Rock Mechanics & Mining Sciences*, v. 41, n. 7, p. 1211-1214, DOI: 10.1016/j.ijrmms.2004.05.001.
- Boulton, S. J., Stokes, M., and Mather, A. E., 2014, Transient fluvial incision as an indicator of active faulting and Plio-Quaternary uplift of the Moroccan High Atlas: *Tectonophysics*, v. 633, p. 16-33, DOI:10.1016/j.tecto.2014.06.032.
- Burbank, D. W., and Anderson, R. S., 2001, *Deformation and Geomorphology at Intermediate Time Scales*, in *Tectonic Geomorphology*: Malden, MA, Blackwell Publishing, 274p.
- DuChene, H., R., and Cunningham, K., I., 2006, Tectonic influences in the Guadalupe Mountains, New Mexico, and Texas: in *Caves and Karst of Southeastern New Mexico*, Land, Lewis; Lueth, Virgil W.; Raatz, William; Boston, Penny; Love, David L.; [eds.], New Mexico Geological Society 57th Annual Fall Field Conference Guidebook, 344 p.
- Duvall, A., Kirby, E., and Burbank, D., 2004, Tectonic and lithologic controls on bedrock channel profiles and processes in coastal California: *Journal of Geophysical Research*, v. 109, n. F3, p. 1-18, DOI: 10.1029/2003JF000086.
- Ellis, M. A., J. B. Barnes, and J. P. Colgan, 2014, Geomorphic evidence for enhanced Pliocene-Quaternary faulting in the northwestern Basin and Range: *Lithosphere*, v. 7, p. 59-72, DOI: 10.1130/L401.1.
- Gao, W., S. P. Grand, W. S. Baldrige, D. Wilson, M. West, J. F. Ni, and R. Aster, 2004, Upper mantle convection beneath the central Rio Grande rift imaged by P and S wave tomography: *Journal of Geophysical Research-Solid Earth*, v. 109, DOI: 10.1029/2003JB002743.
- Happel, A., 2017, Evaluating fault-line escarpment exposure in the Guadalupe Mountains of Texas and West Mexico, Manuscript in preparation.
- Hawley, J. W., 1993b, The Ogallala and Gatuña Formations in the southeastern New Mexico region, a progress report; in Love, D. W., Hawley, J. W., Kues, B. S., Adams, J. W., Austin, G. S., and Barker, J. M. (eds.), *Carlsbad region, New Mexico and west Texas*: New Mexico Geological Society, Guidebook 44, p. 261-269.



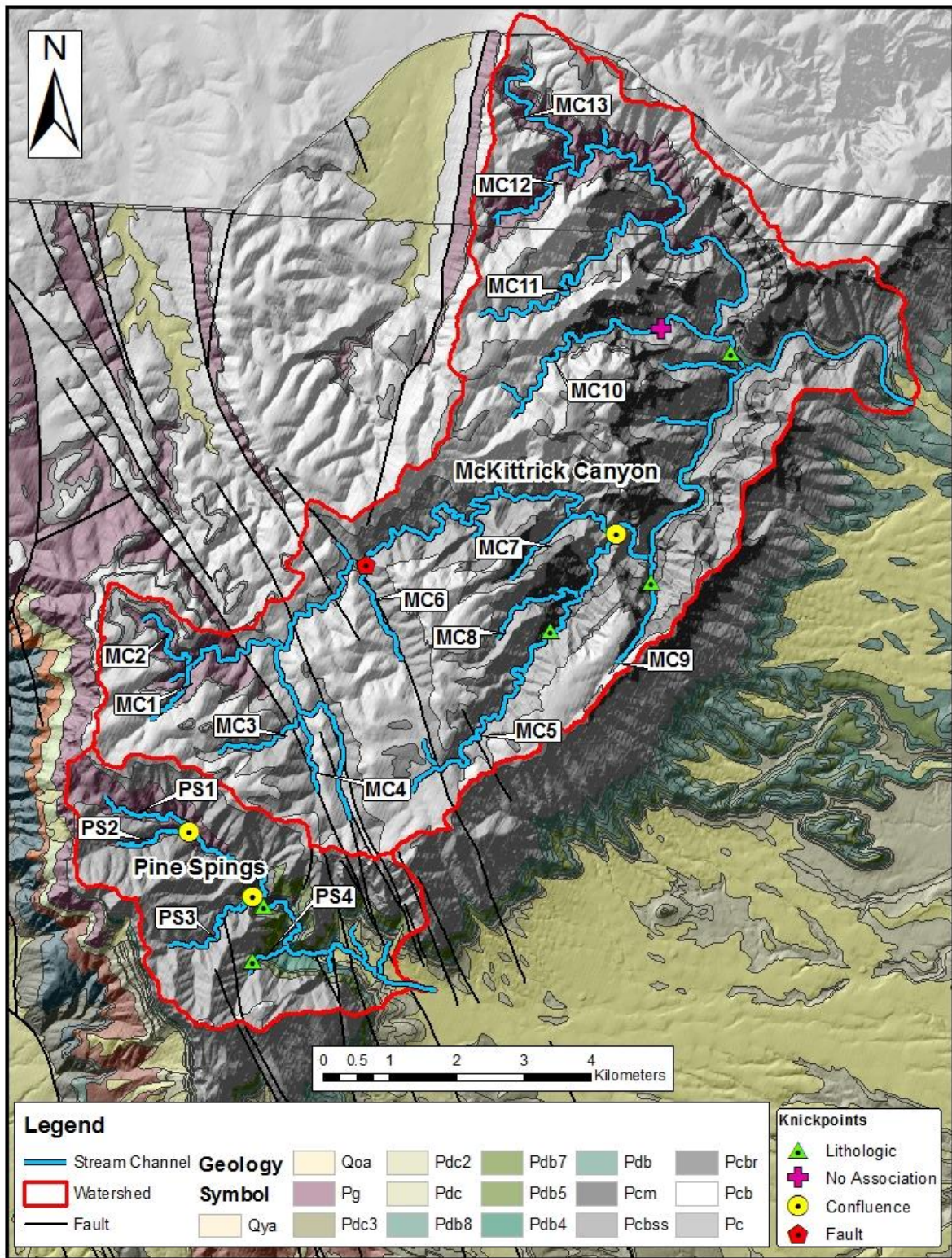
- Hoffman, L. L., 2014, Spatial variability of erosion patterns along the eastern margin of the Rio Grande Rift [MS thesis]: Illinois State University, 61 p.
- King, P. B., 1948, Geology of the southern Guadalupe Mountains, Texas: U.S. Geological Survey Professional Paper 215, map scale 1:48000.
- Kirby, E., and Whipple, K., 2001, Quantifying differential rock-uplift rates via stream profile analysis: *Geology*, v. 29, p. 415-418, DOI: 10.1130/0091-7613(2001)029<0415:QDRURV>2.0.CO;2,.
- Kosa, E., and Hunt, D., 2006, The effect of syndepositional deformation within the Upper Permian Capitan Platform on the speleogenesis and geomorphology of the Guadalupe Mountains, New Mexico, USA: *Geomorphology*, v. 78, n. 3-4, p. 279-308, DOI: 10.1016/j.geomorph.2006.01.038.
- Larson, I. J., and Montgomery, D. R., 2012, Landslide coupled to tectonics and river incision: *Nature Geoscience*, v. 5, n. 7, p. 468-473, DOI: 10.1038/ngeo1479.
- Lifton, Z. M., Thackray, G. D., Kirk, R. V., Glenn, N. F., 2009, Influence of rock strength on the valley morphometry of Big Creek, central Idaho, USA; *Geomorphology*, v. 11, no. 3-4, DOI: 10.1016/j.geomorph.2009.04.014.
- Lu, P., and Shang, Y., 2015, Active tectonic revealed by river profiles along the Popu Fault: *Water*, v. 7, n. 4, p. 1628-1648, DOI: 10.3390/w7041628.
- Miller, S. R., Sak, P. B., Kirby, E., and Bierman, P. R., 2013, Neogene rejuvenation of central Appalachian topography: Evidence for differential uplift from stream profiles and erosion rates: *Earth and Planetary Science Letters*, v. 1, n. 12, p. 369-370, DOI: 10.1016/j.epsl.2013.04.007.
- Montgomery, D. R., and Brandon, M. T., 2002, Topographic controls on erosion rates in tectonically active mountain ranges: *Earth and Planetary Science Letters*, v. 201, n. 3-4, p. 481-489, DOI: 10.1016/S0012-821X(02)00725-2.
- Moore, J. R., Sanders, J. W., Dietrich, W. E., and Glaser, S. D., 2009, Influence of rock mass strength on the erosion rate of alpine cliffs: *Earth Surface Processes and Landforms*, v. 34, p. 1339-1352, DOI: 10.1002/esp.1821.
- Moon, V., Russell, G., and Stewart, M., 2001, The value of rock mass classification systems for weak rock masses: a case example from Huntly, new Zealand: *Engineering Geology*, v. 61, p. 57-63, DOI: 10.1016/S0013-7952(01)00024-2.
- Ouimet, W., Whipple, K. X., and Granger, D., 2009, Beyond threshold hillslopes: Channel adjustment to base-level fall in tectonically active mountain ranges: *Geology*, v. 37, n. 7, p. 579-582, DOI: 10.1130/G30013A.1.
- Reid, I., Laronne, J. B., Powell, M. D., 1998, Flash-flood and bedload dynamics of desert gravel-bed stream: *Hydrological Processes*, v. 12, p. 543-557, DOI: 10.1002/(sici)1099-1085(19980330)12:4<543::aid-hyp593>3.0.co;2-c

- Ritter, D. F., Kochel, R. C., and Miller, J. R., 2011, *Fluvial Processes*, fifth edition, in *Process Geomorphology*: Long Grove, IL, Waveland Press Inc., 652p.
- Rockett, C., Pulliam, R., 2011, *Seismic Tomographic Imaging Reveals Possible Lithospheric Erosion beneath Trans-Pecos Texas and Southeastern New Mexico* [MS Thesis]: Baylor University, 85 p.
- Selby, M. J., 1980, A rock mass strength classification for geomorphic purposes: with tests from Antarctica and New Zealand. *Zeitschrift für Geomorphologie*, v. 24, no. 1, p. 31-51.
- Selby, M. J., 1982, Controls on the stability and inclinations of hillslopes formed of hard rock: *Earth Surface Processes and Landforms*, v. 7, no. 5, DOI: 10.1002/esp.3290070506.
- Scholle, P. A., and Halley, R. B., 1980, Upper Paleozoic depositional and diagenetic facies in a mature petroleum province (A field guide to the Guadalupe and Sacramento Mountains): USGS Open-File Report 80-383, 191 p.
- Sklar, L. S., and Dietrich, W. E., 2001 Sediment and rock strength controls on river incision into bedrock: *Geology*, v. 29, n. 12, p. 1087-1090, DOI:10.1130/0091-7613(2001)029<1087:SARSCO>2.0.CO.
- Snyder, N., Whipple, K., Tucker, G., Merretts, D., 2000, Stream profiles in the Mendocino triple junction region, northern California: *GSA Bulletin*, v. 112, n. 8, p. 1250-1263, DOI: 10.1130/0016-7606(2000)112<1250:Irttfd>2.3.co;2.
- Standen, A., Finch, S., Williams, R., Lee-Brand, B., and Kirby, P., 2009, Capitan Reef Complex Structure and Stratigraphy: Texas Water Development Board open file report 0804830794, 53 p.
- Viles, H., Goudie, A., Grab, S., and Lalley, J., 2011, The use of the Schmidt Hammer and Equotip for rock hardness assessment in geomorphology and heritage science: a comparative analysis: *Earth Surface Processes and Landforms*, v. 36, n. 3, p. 320-333, DOI: 10.1002/esp.2040.
- Ward, P. L., 1991, On plate-tectonics and the geologic evolution of southwestern North-America: *Journal of Geophysical Research-Solid Earth and Planets*, v. 96, p. 12479-12496, DOI: 10.1029/91JB00606.
- Whipple, K., X., 1999, Dynamics of the stream-power river incision model: Implications for height limits of mountains ranges, landscape response timescales, and research needs: *Journal of Geophysical Research*, v. 104, p. 661-674, DOI: 10.1029/1999JB900120.
- Whipple, K., X., 2004, Bedrock rivers and the geomorphology of active orogens: *Annual Review of Earth and Planetary Sciences*, v. 32, n. 1, p. 151-185, DOI: 10.1146/annurev.earth.32.101802.120356.
- Wobus, C., Whipple, K. X., Kirby, E., Snyder, N. P., Johnson, J., Spyropolou, K., Crosby, B., and Sheehan, D., 2006, Tectonics from topography: Procedures, promise, and pitfalls: *Tectonics, Climate, and Landscape Evolution*, v. 398, p. 55-74.

Woodside, J., Peterson, E., W., and Dogwiler, T., 2015, Longitudinal profile and sediment mobility as geomorphic tools to interpret the history of a fluviokarst stream system: *International Journal of Speleology*, v. 44, n. 2, p. 197-206, DOI: <http://dx.doi.org/10.5038/1827-806X.44.2.9>.

Yang, R., Willett, S. D., and Goren, L., 2015, In situ low-relief landscape formation as a result of river network disruption: *Nature*, v. 520, n. 7548, p. 526-529, DOI: 10.1038/nature14354.













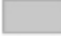
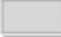


# APPENDIX A: STUDY SITE WITH KNICKPOINTS, SAMPLE SITES, AND GEOLOGY



## APPENDIX B: KING'S 1948 GEOLOGIC MAP SYMBOLS KEY

### Geology

#### Symbol

	Qya	Quaternary Alluvium:
	Qoa	<i>young (y) and old (o)</i>
	Pg	Goat Seep limestone
	Pdc3	Cherry Canyon formation:
	Pdc2	
	Pdc	
	Pdb8	Bell Canyon formation:
	Pdb7	
	Pdb5	
	Pdb4	
	Pdb	
	Pcm	Capitan limestone:
	Pcbr	<i>Brecciated (br),</i>
	Pc	<i>and Massive (m)</i>
	Pcb	Carlsbad Limestone:
	Pcbss	<i>Sandstone (ss)</i>

Modified from King (1948)

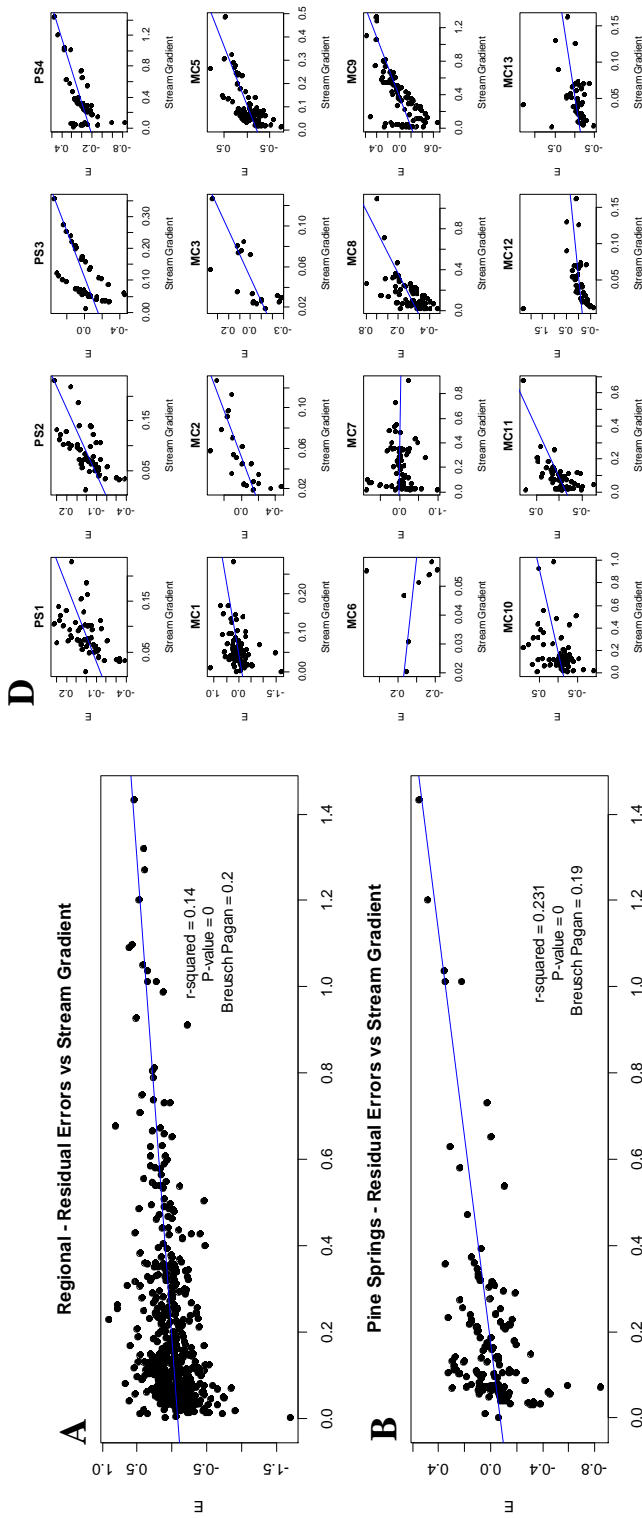


## APPENDIX C: MASTER REBOUND TABLES

Appendix 1 Master Rebound Data															
Sample ID	Sample	Latitude WGS84	Longitude WGS84	Lithology	Formation	Corrected Rebound	Polished Measure d Rebound	STD V	Sample Strike s (n)	Total Strike s (#)	Angle	Integrated Rebound	STD V	n	RMS Total Rating
PSRS01	1	31.89972	-104.84167	skeletal limestone	Bell Canyon Hegler	64.6	64.6	5.3	10	1522	side	54.8	10.1	20	78
PSRS02	2	31.90194	-104.84111	skeletal limestone	Bell Canyon Hegler	71.8	71.8	2.9	10	1542	side	68.6	3.3	20	73
PSRS03	3	31.90194	-104.84750	cherty limestone	Bell Canyon Hegler	68.0	68.0	3.5	12	1567	side	70.7	3.0	22	63
PSRS04	4	-	-	sandstone	Bell Canyon SS	29.5	29.5	1.9	12	1591	side	30.3	0.8	24	-
PSRS05	5	31.90333	-104.84778	limestone	Bell Canyon Hegler	52.3	52.3	1.2	10	1613	side	52.6	0.3	20	69
PSRS06	6	31.90500	-104.84639	brecciated limestone	Bell Canyon Pinery	71.0	71.0	1.4	10	1659	side	67.8	3.3	20	86
PSRS07	7	31.90389	-104.84778	brecciated limestone	Bell Canyon Hegler	57.8	57.8	3.3	10	1678	side	58.8	1.1	19	-
PSRS08	8	31.90028	-104.83583	sandstone	Cherry Canyon SS	64.5	64.5	3.0	10	1698	side	60.0	4.6	20	67
PSRS09	9	31.90734	-104.85213	brecciated limestone	Capitan Brecciated	61.6	61.6	4.4	10	1738	side	63.8	2.3	20	72
PSRS10	10	31.91306	-104.85861	massive limestone	Capitan Limestone	56.1	56.1	1.9	10	1764	side	55.9	0.2	20	66
PSRS11	11	31.91056	-104.85194	brecciated limestone	Capitan Brecciated	69.8	69.8	3.4	10	1784	side	64.1	5.8	20	-
PSRS12	12	31.89194	-104.88250	brecc/massive lmstne	Goat Seep	67.0	67.0	2.9	10	1804	side	66.6	0.4	20	-
MCRS01	13	31.97972	-104.75639	sandstone	Bell Canyon SS	62.5	60.5	1.7	10	1824	top	62.3	0.2	20	89
MCRS02	14	31.96639	104.78833	fossiliferous limstne	Capitan Limestone	60.7	60.7	2.9	10	1854	side	61.1	0.4	20	78
MCRS03	15	31.96556	104.78778	fossiliferous limstne	Bell Canyon Hegler	75.3	75.3	1.9	10	1884	side	72.1	3.3	20	73
MCRS04	16	31.96083	104.79278	fossiliferous limstne	Capitan Limestone	60.5	60.5	3.2	10	1924	side	59.5	1.1	20	75
MCRS05	17	-	-	brecciated limestone	Capitan Brecciated	60.5	60.5	4.9	10	1924	side	59.5	1.1	20	-
MCRS06	18	-	-	brecciated limestone	Capitan Brecciated	72.0	72.0	3.6	10	1944	side	66.5	5.6	20	-
MCRS07	19	31.98333	104.77806	fossiliferous limstne	Capitan Limestone	75.0	75.0	1.1	10	2006	side	72.3	2.8	20	81
MCRS08	20	31.98333	104.77778	massive limestone	Capitan Limestone	69.9	69.9	3.1	10	2026	side	65.4	4.6	20	89
MCRS09	21	31.98694	104.75861	massive limestone	Capitan Massive	72.5	70.4	1.8	10	2046	top	70.5	2.1	20	83
NMCRS01	22	31.02028	104.81667	sandstone	Carlsbad Sandstone	68.5	67.7	2.4	10	2091	top	62.5	6.2	20	81
NMCRS02	23	31.02222	104.81778	limestone	Goat Seep	67.0	67.0	2.2	10	2011	side	65.5	1.5	20	73
NMCRS03	24	31.02333	104.81528	limestone	Carlsbad Limestone	69.5	69.5	3.5	10	2131	side	62.5	7.2	20	70
					Average							62.0	8.9	485	

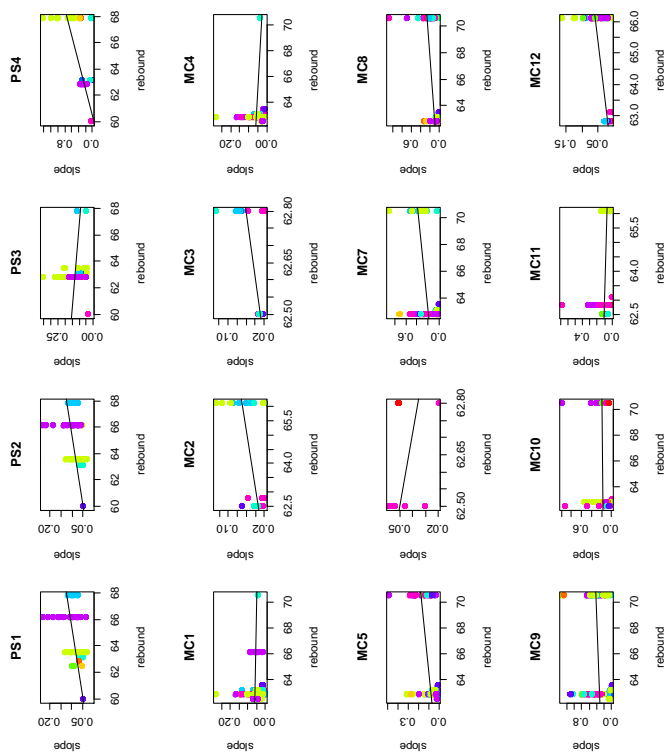
Appendix 1 Master Rebound Data															
Sample ID	Sample	Latitude WGS84	Longitude WGS84	Lithology	Formation	Corrected Rebound	Unpolished Measured Rebound	STD V	Sample Strikes (n)	Total Strikes (#)	Angle	Integrated Rebound	STD V	n	RMS Total Rating
PSRS01	1	31.89972	-104.84167	skeletal limestone	Bell Canyon Hegler	44.9	44.9	8.0	10	1512	side	54.8	10.1	20	78
PSRS02	2	31.90194	-104.84111	skeletal limestone	Bell Canyon Hegler	65.3	65.3	5.7	10	1532	side	68.6	3.3	20	73
PSRS03	3	31.90194	-104.84750	cherty limestone	Bell Canyon Hegler	73.9	73.9	2.9	10	1552	side	70.7	3.0	22	63
PSRS04	4	-	-	sandstone	Bell Canyon SS	31.1	31.1	4.0	12	1579	side	30.3	0.8	24	-
PSRS05	5	31.90333	-104.84778	limestone	Bell Canyon Hegler	52.8	52.8	2.1	10	1603	side	52.6	0.3	20	69
PSRS06	6	31.90500	-104.84639	brecciated limestone	Bell Canyon Pinery	64.5	64.5	3.4	10	1649	side	67.8	3.3	20	86
PSRS07	7	31.90389	-104.84778	brecciated limestone	Bell Canyon Hegler	60.0	6.1	6.1	9	1669	side	58.8	1.1	19	-
PSRS08	8	31.90028	-104.83583	sandstone	Cherry Canyon SS	55.5	55.5	3.2	10	1688	side	60.0	4.6	20	67
PSRS09	9	31.90734	-104.85213	brecciated limestone	Capitan Brecciated	66.0	66.0	3.1	10	1708	side	63.8	2.3	20	72
PSRS10	10	31.91306	-104.85861	massive limestone	Capitan Limestone	55.7	55.7	6.2	10	1748	side	55.9	0.2	20	66
PSRS11	11	31.91056	-104.85194	brecciated limestone	Capitan Brecciated	58.4	58.4	5.0	10	1774	side	64.1	5.8	20	-
PSRS12	12	31.89194	-104.88250	brecc/massive limestone	Goat Seep	66.2	66.2	6.5	10	1794	side	66.6	0.4	20	-
MCRS01	13	31.97972	-104.75639	sandstone	Bell Canyon SS	62.1	60.1	2	10	1814	top	62.3	0.2	20	89
MCRS02	14	31.96639	104.78833	fossiliferous limestone	Capitan Limestone	61.4	61.4	3.5	10	1834	side	61.1	0.4	20	78
MCRS03	15	31.96556	104.78778	fossiliferous limestone	Bell Canyon Hegler	68.8	68.8	2.7	10	1874	side	72.1	3.3	20	73
MCRS04	16	31.96083	104.79278	fossiliferous limestone	Capitan Limestone	58.4	58.4	4.9	10	1914	side	59.5	1.1	20	75
MCRS05	17	-	-	brecciated limestone	Capitan Brecciated	58.4	58.4	4.9	10	1914	side	59.5	1.1	20	-
MCRS06	18	-	-	brecciated limestone	Capitan Brecciated	61.0	61.0	4.5	10	1934	side	66.5	5.6	20	-
MCRS07	19	31.98333	104.77806	fossiliferous limestone	Capitan Limestone	69.6	69.6	2.3	10	1974	side	72.3	2.8	20	81
MCRS08	20	31.98333	104.77778	massive limestone	Capitan Limestone	60.9	60.9	4.2	10	2016	side	65.4	4.6	20	89
MCRS09	21	31.98694	104.75861	massive limestone	Capitan Massive	68.5	67.8	3.3	10	2036	top	70.5	2.1	20	83
NMCRS01	22	31.02028	104.81667	sandstone	Carlsbad Sandstone	56.5	57.8	1.7	10	2081	top	62.5	6.2	20	81
NMCRS02	23	31.02222	104.81778	limestone	Goat Seep	64.0	64.0	2.4	10	2101	side	65.5	1.5	20	73
NMCRS03	24	31.02333	104.81528	limestone	Carlsbad Limestone	55.4	55.4	4	10	2121	side	62.5	7.2	20	70
Average												62.0	8.9	485	

# APPENDIX D: STREAM GRADIENT VS FLINT'S LAW RESIDUAL ERRORS

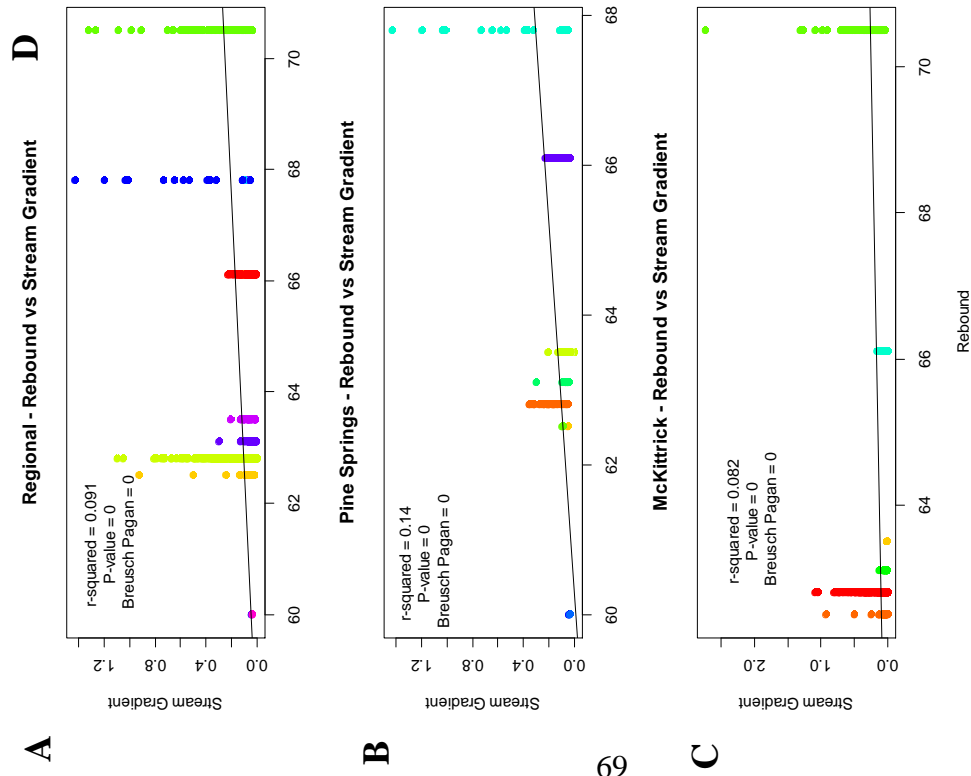


Appendix C: Simple regression analyses between  
 Flints Law residual errors and channel gradient  
 (slope) (A) regionally, in (B) Pine Springs Canyon,  
 (C) McKittrick Canyon, and (D) individual streams.

APPENDIX E: REBOUND VS STREAM GRADIENT W/ SCATTER

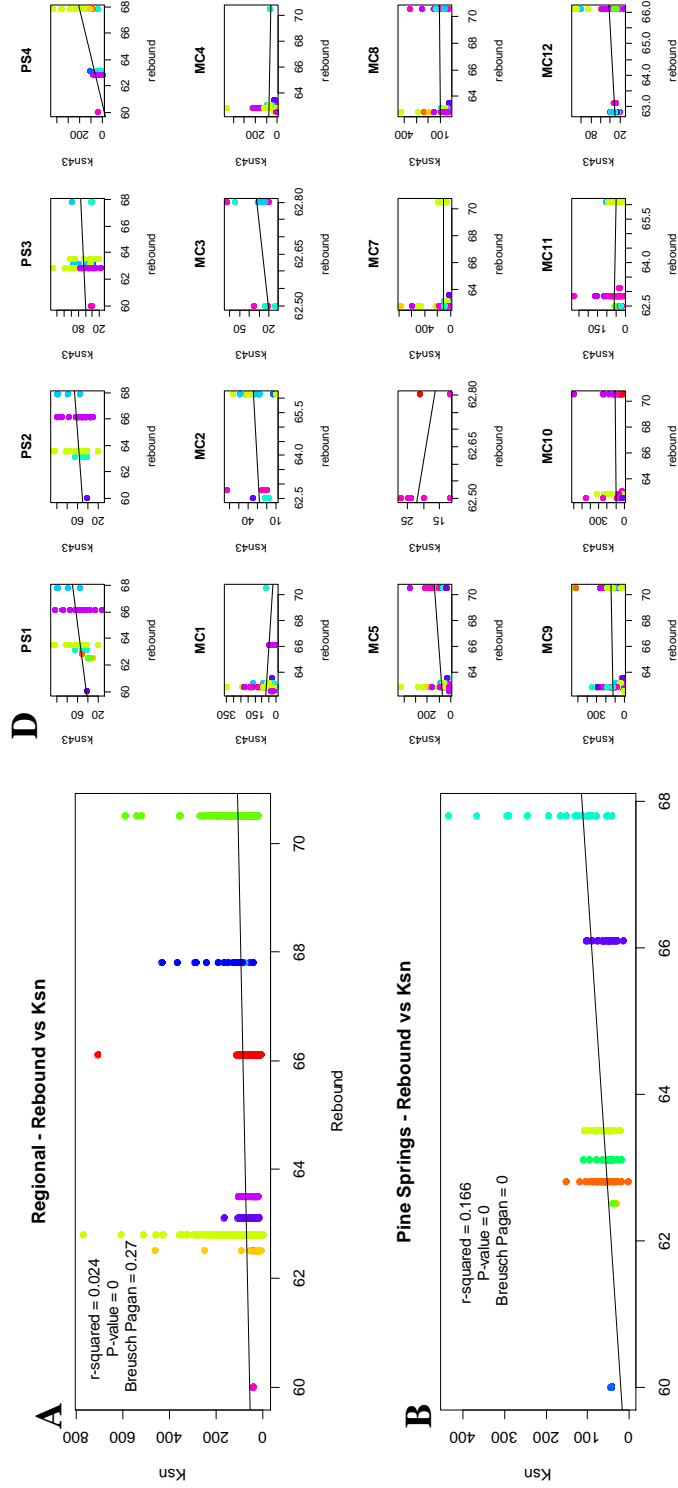


Appendix D: Simple regression analyses between rebound and stream gradient (slope) (A) regionally, in (B) Pine Springs canyon, (C) McKittrick Canyon, and (D) individual rivers.



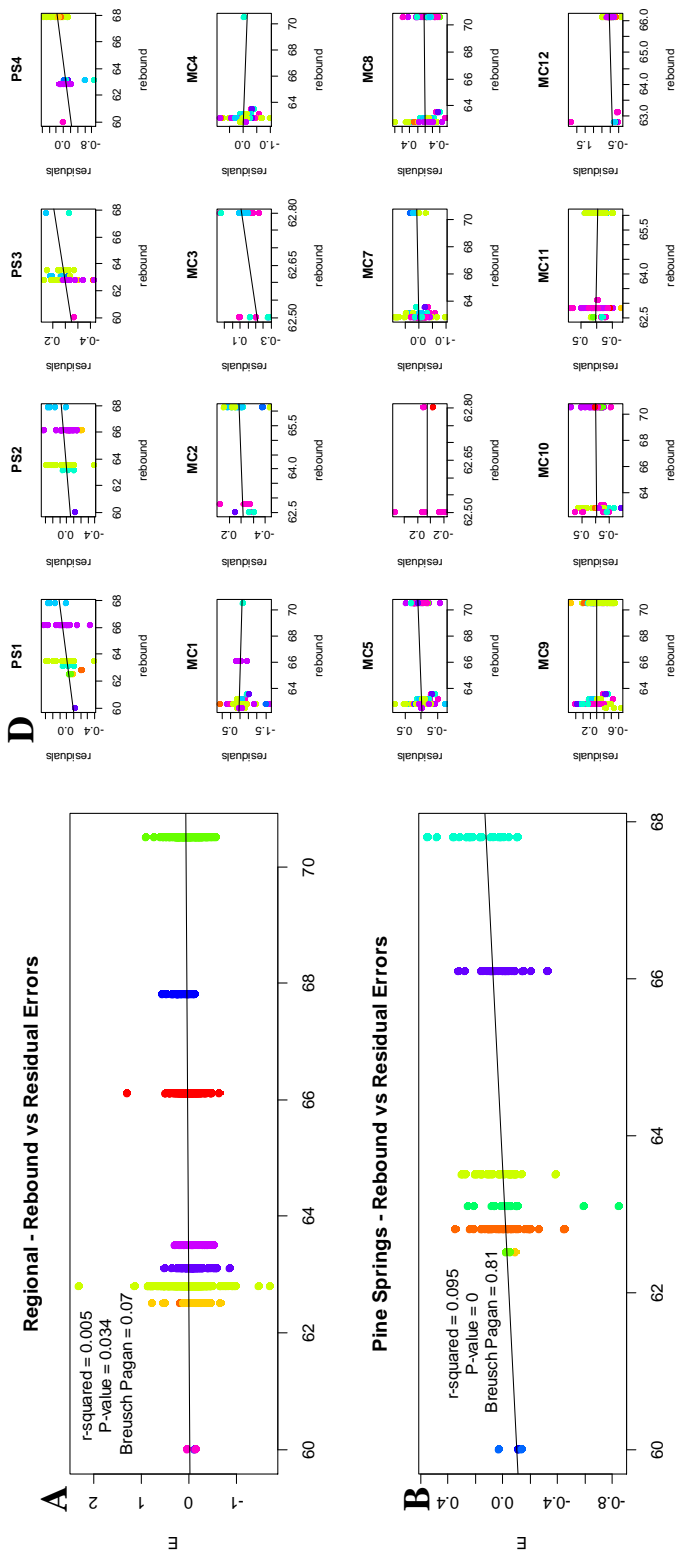


## APPENDIX F: REBOUND VS $K_{SN}$ W/ SCATTER

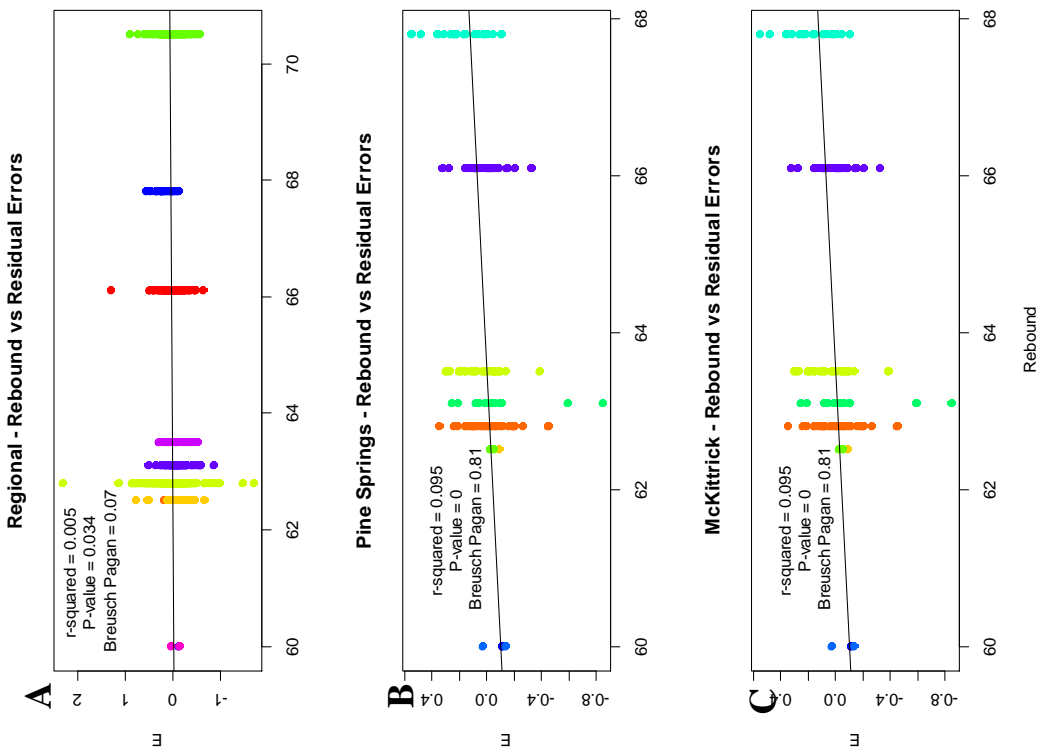


Appendix E: Simple regression analyses between rebound and  $K_{sn}$  (A) regionally, in (B) Pine Springs Canyon, (C) McKittrick Canyon, and (D) individual streams.

APPENDIX G: REBOUND VS FLINT'S LAW RESIDUAL ERROR W/ SCATTER



Appendix F: Simple regression analyses between rebound and Flint's Law residual errors (A) regionally, in (B) Pine Springs Canyon, (C) McKittrick Canyon, and (D) individual streams.



## APPENDIX H: STREAM DELINEATION STEPS IN GIS (VER. 10)

